

Montana Tech Library

Digital Commons @ Montana Tech

---

Graduate Theses & Non-Theses

Student Scholarship

---

Spring 5-2023

## THE USE OF NOVEL CEMENT ADDITIVES TO INCREASE THE CARBON STORAGE POTENTIAL OF OILFIELD CEMENTS

Rob Braden

Follow this and additional works at: [https://digitalcommons.mtech.edu/grad\\_rschn](https://digitalcommons.mtech.edu/grad_rschn)

---

### Recommended Citation

Braden, Rob, "THE USE OF NOVEL CEMENT ADDITIVES TO INCREASE THE CARBON STORAGE POTENTIAL OF OILFIELD CEMENTS" (2023). *Graduate Theses & Non-Theses*. 307.  
[https://digitalcommons.mtech.edu/grad\\_rschn/307](https://digitalcommons.mtech.edu/grad_rschn/307)

This Thesis is brought to you for free and open access by the Student Scholarship at Digital Commons @ Montana Tech. It has been accepted for inclusion in Graduate Theses & Non-Theses by an authorized administrator of Digital Commons @ Montana Tech. For more information, please contact [sjuskiewicz@mtech.edu](mailto:sjuskiewicz@mtech.edu).

THE USE OF NOVEL CEMENT ADDITIVES TO INCREASE THE  
CARBON STORAGE POTENTIAL OF OILFIELD CEMENTS

by  
Robb Braden

A thesis submitted in partial fulfillment of the  
requirements for the degree of

Master of Science in Petroleum Engineering

Montana Technological University

2023



## Abstract

The topic of carbon sequestration has become increasingly popular in recent years as a solution to combat the increasing amounts of carbon dioxide in Earth's atmosphere. Various industries have researched methods in which to implement carbon sequestration projects to offset the carbon dioxide emissions associated with their operations. The U.S. oil and gas exploration industry in particular has seen multi-billion-dollar investments by multiple firms into carbon sequestration and emission reduction projects. The largest single industrial emitter of carbon dioxide into the atmosphere currently is the production of cement, which accounts for 8% of all global industrial carbon dioxide emission (Ellis et al., 2020). The oil and gas exploration industry utilizes cement when constructing new oil and natural gas wells and also when plugging and abandoning wells. These cementing operations present an opportunity to store and sequester carbon by entrapping carbon-laden materials in the cement slurry, which would permanently store the carbon in the subsurface. This application of carbon sequestration would offset some of the emissions associated with the use of cement in oil and gas industry operations. This study examines three novel waste materials proposed as oilfield cement additives. These materials were selected due to their associated carbon sequestration capabilities. These three materials are hemp hurd, biochar, and non-recyclable plastic.

The three novel materials proposed in this study were examined as additives in a typical oil field cement design. Early compressive strength, slurry density, and rheological properties were determined for varying concentrations of these materials added to common oil field cement slurries.

Hemp hurd was found to add early compressive strength to the cement design. This increase was hypothesized to be caused by accelerated cement hydration caused by addition of the material into the design. Pumpability was identified as a potential concern regarding the use of the material as a cement additive as addition of the material caused a large increase in the cement slurry apparent viscosity. Biochar was also found to add early compressive strength attributes to the cement design. This increase was also hypothesized to be caused by accelerated cement hydration. Biochar also proved to be easily mixed at very high additive rates into the cement design without producing pumpability issues. Non-recyclable plastic was found to have very high rates of carbon sequestration by mass in the cement designs while not having a significant effect on the cement design's early compressive strength and rheology. The use of these novel materials in a primary well cementing operation at an additive rate of 2.0 pounds per sack of cement could sequester between 3,400-11,600 pounds of carbon dioxide equivalent in the wellbore cement.

Keywords: Carbon Sequestration, Early Compressive Strength, Accelerated Cement Hydration, Hemp Hurd, Biochar, Non-Recyclable Plastic

## **Dedication**

I wish to thank my mother Vicki, my father Brad, and my brother Samuel for their continued support and love through my time on this research. Without you, I would have never gotten the opportunity to pursue this degree and complete this work!

## **Acknowledgements**

I would like to thank my advisor Dr. Lee Richards for his guidance and input throughout this project. Committee members Dr. Burt Todd and Dr. John Robertson for their valuable feedback and support. The Montana Tech Petroleum Department for providing the funding for this research. The Montana Tech Petroleum Department faculty for providing feedback on my research. IND Hemp for providing the hemp hurd for this study. Miller Soils for providing the biochar for this study. GCC Trident Plant for providing the cement for this study.

## Table of Contents

<b>ABSTRACT .....</b>	<b>II</b>
<b>LIST OF TABLES.....</b>	<b>IX</b>
<b>LIST OF FIGURES.....</b>	<b>X</b>
<b>GLOSSARY OF TERMS .....</b>	<b>XIII</b>
<b>1. INTRODUCTION .....</b>	<b>1</b>
<b>1.1. Carbon Emission and Global Warming .....</b>	<b>1</b>
1.1.1. Global Climate Change .....	2
<b>1.2. Carbon Emission Reduction Investments in the Oil and Gas Industry.....</b>	<b>3</b>
<b>1.3. Carbon Emissions Associated with Cement Production .....</b>	<b>3</b>
<b>1.4. Cement in the Oil and Gas Industry.....</b>	<b>4</b>
<b>1.5. Carbon Sequestration.....</b>	<b>5</b>
<b>1.6. Hemp Hurd .....</b>	<b>6</b>
<b>1.7. Biochar .....</b>	<b>7</b>
<b>1.8. Non-Recyclable Plastics.....</b>	<b>7</b>
<b>2. LITERATURE REVIEW.....</b>	<b>9</b>
<b>2.1. Hemp Hurd as a Concrete Additive .....</b>	<b>9</b>
<b>2.2. Biochar as a Concrete Additive .....</b>	<b>10</b>
<b>2.3. Recycled Plastic as a Concrete Additive .....</b>	<b>11</b>
<b>3. MATERIALS AND METHODS .....</b>	<b>15</b>
<b>3.1. Experimental Approach.....</b>	<b>15</b>
3.1.1. Overview .....	15
3.1.2. Base Cement Design.....	17
3.1.3. Modified Cement Design .....	18
3.1.4. Establishing a Control.....	20

3.2.	<i>Materials</i> .....	21
3.2.1.	Cement.....	21
3.2.2.	Calcium Chloride Additive .....	22
3.2.3.	Freshwater Additive .....	23
3.2.4.	Hemp Hurd .....	23
3.2.4.1.	1-20 Hemp Hurd.....	23
3.2.4.2.	1-16 Hemp Hurd.....	25
3.2.5.	Biochar .....	27
3.2.6.	Non-Recyclable Plastic .....	29
3.3.	<i>Methods</i> .....	31
3.3.1.	Additive Size Distribution Quantification Using a Sieve .....	32
3.3.1.1.	Additive Size Distribution Quantification Procedure.....	33
3.3.2.	Preparation of Cement Slurry.....	34
3.3.2.1.	Preparation of Cement Slurry Procedure (Based on API RP 10B-2) .....	34
3.3.3.	Determination of Cement Sample Slurry Density Using a Mud Balance .....	35
3.3.3.1.	Determination of Cement Sample Slurry Density Procedure (Based on API RP 10B-2) .....	36
3.3.4.	Determination of Cement Slurry Rheological Properties Using a Rotational Viscometer .....	36
3.3.4.1.	Determination of Cement Slurry Rheological Properties Procedure (based on API RP 10B-2) .	37
3.3.5.	Creating Sample Molds for Unconfined Compressive Strength Testing.....	38
3.3.5.1.	Creating Sample Molds for Unconfined compressive Strength Testing Procedure (based on API RP 10B-2)	39
3.3.6.	Testing Cement Samples for Unconfined Compressive Strength .....	40
3.3.6.1.	Testing Samples for Unconfined Compressive Strength Procedure (based on API RP 10B-2) ..	41
3.4.	<i>Materials and Methods Conclusion</i> .....	42
4.	RESULTS.....	43
4.1.	<i>Unconfined Compressive Strength Results</i> .....	43
4.1.1.	Control Group Unconfined Compressive Strength Results.....	44
4.1.2.	Hemp Hurd Additive Unconfined Compressive Strength Results.....	45
4.1.3.	Biochar Additive Unconfined Compressive Strength Results .....	49

4.1.4.	Non-Recyclable Plastic Unconfined Compressive Strength Results .....	52
4.2.	<i>Rheological Testing Results</i> .....	55
4.2.1.	Control Group Rheological Testing Results .....	55
4.2.2.	Hemp Hurd Rheological Testing Results.....	57
4.2.3.	Biochar Rheological Property Testing Results .....	59
4.2.4.	Non-Recyclable Plastic Rheological Testing Results .....	61
5.	DISCUSSION AND CONCLUSIONS .....	65
5.1.	<i>Analysis of Unconfined Compressive Strength Results</i> .....	65
5.1.1.	Hemp Hurd Additive Unconfined Compressive Strength Analysis .....	65
5.1.2.	Biochar Additive Unconfined Compressive Strength Analysis.....	66
5.1.3.	Non-Recyclable Plastic Additive Unconfined Compressive Strength Analysis.....	67
5.2.	<i>Analysis of Rheological Effects of the Novel Cement Additives</i> .....	67
5.2.1.	Effects of Novel Cement Additives on Pump Pressure during a Primary Cementing Operation .....	69
5.3.	<i>Carbon Sequestration Potential of Novel Cement Additives</i> .....	70
5.4.	<i>Potential of Proposed Novel Materials as Oilfield Cement Additives</i> .....	72
5.4.1.	Hemp Hurd .....	72
5.4.2.	Biochar .....	72
5.4.3.	Non-Recyclable Plastic .....	73
6.	CONCLUSIONS OVERVIEW.....	74
7.	RECOMMENDATIONS FOR FUTURE WORK.....	75
7.1.	<i>Unconfined Compressive Strength Testing at Reservoir Temperature and Pressure</i> .....	75
7.2.	<i>Thickening Time Testing</i> .....	75
7.3.	<i>Long-Term Compressive Strength Testing</i> .....	76
7.4.	<i>Lost Circulation Material (LCM) Capability Testing</i> .....	76
7.5.	<i>Investigation of Thermal Conductivity Effects of the Non-Recyclable Plastic Novel Cement Additive</i>	
	77	
8.	RECOMMENDED FUTURE WORK OVERVIEW.....	78
9.	APPENDIX A: UNCONFINED COMPRESSIVE STRENGTH RESULTS .....	83



10. APPENDIX B: WATER REQUIREMENT CALCULATION FOR CONTROL GROUP EXPERIMENTS ..... 92

**WATER REQUIREMENT CALCULATION EXAMPLE..... 93**

11. APPENDIX C: 100 RPM APPARENT VISCOSITY AND GEL STRENGTH RESULTS..... 95

**List of Tables**

Table 1 - Base Cement Design.....	18
Table 2 - Modified Cement Design .....	19
Table 3 - Control Cement Design .....	20
Table 4: 1-20 Hemp Hurd Additive Size Distribution.....	25
Table 5: 1-16 Hemp Hurd Additive Size Distribution.....	27
Table 6: Biochar Additive Size Distribution .....	29

## List of Figures

Figure 1: Carbon dioxide emissions and atmospheric concentration from 1750-2020 (NOAA, 2021) .....	2
Figure 2: Schematic diagram for primary oil well cementing (Mtaki et al., 2020) .....	4
Figure 3: Simplified illustration of a typical offshore production well before and after P&A (Vrålstad et al., 2019).....	5
Figure 4: Recycling process of PE and PET wastes (Tayeh et al., 2021).....	12
Figure 5: Types of Recycled Plastic Additive used as replacement of natural coarse aggregates: (a) Granules, (b) Fibers, (c) Black flakes, (d) Mixed flakes, and (e) White Flakes. (Basha et al., 2020) .....	13
Figure 6 : 94-97% Calcium Chloride Mini-Pellets Picture.....	22
Figure 7: Picture of 1-20 Hemp Hurd Material .....	24
Figure 8: Picture of 1-16 Hemp Hurd Material .....	26
Figure 9: Picture of Biochar Material Used During Experimentation .....	28
Figure 10: Diagram of Six Pack can Holder with Initial Cut Marks .....	30
Figure 11: Picture of Non-Recyclable Plastic Material Used During Experimentation....	31
Figure 12: Retsch Model AS 200 Vibrating Sieve .....	33
Figure 13: Picture of a Fann Model 35A Rotary Viscometer.....	37
Figure 14: Picture of Humboldt Model H-2820 Cement Mold .....	39
Figure 15: Picture of Carver Hydraulic Unit Model #3912.....	41
Figure 16: Control Group 12 Hour Compressive Strength Results .....	45
Figure 17: Hemp Hurd 12-Hour Compressive Strength vs. Additive Rate Chart .....	47
Figure 18: Hemp Hurd 12 Hour Compressive Strength vs. Slurry Density Chart .....	48

Figure 19: Biochar 12 Hour Compressive Strength vs. Additive Rate Chart.....	50
Figure 20: Biochar 12 Hour Compressive Strength vs. Slurry Density Chart.....	51
Figure 21: Non-recyclable Plastic 12 Hour Compressive Strength vs. Additive Rate Chart	53
Figure 22: Non-Recyclable Plastic 12 Hour Compressive Strength vs. Slurry Density Chart .....	54
Figure 23: Control Group Slurry Apparent Viscosity vs. Measured Density (@100 RPM)	56
Figure 24: Control Group Gel Strength vs. Measured Density Chart.....	57
Figure 25: Hemp Hurd Slurry Apparent Viscosity vs. Measured Density (@100 RPM) .	58
Figure 26: Hemp Hurd Additive Gel Strength vs. Measured Density .....	59
Figure 27: Hemp Hurd Additive Gel Strength vs. Measured Density Chart .....	59
Figure 28: Biochar Slurry Apparent Viscosity vs. Measured Density (@ 100 RPM).....	60
Figure 29: Biochar Additive Gel Strength vs. Measured Density .....	61
Figure 30: Non-Recyclable Plastic Slurry Apparent Viscosity vs. Measured Density (@100 RPM).....	62
Figure 31: Biochar Additive Gel Strength vs. Measured Density .....	63
Figure 32: Carbon Sequestration Potential of Novel Cement Additives .....	71

**List of Equations**

(1) Apparent Viscosity Equation .....	55
---------------------------------------	----

## Glossary of Terms

<b>Term</b>	<b>Definition</b>
Anthropogenic	(chiefly of environmental pollution and pollutants) originating in human activity.
Apparent Viscosity	The shear stress applied to a fluid divided by the shear rate.
Carbon Dioxide Equivalent (CO <sub>2e</sub> )	The number of tons of carbon dioxide emissions with the same global warming potential as one ton of another greenhouse gas.
Casing	A series of steel pipes that are run into a drilled hydrocarbon well to stabilize the well, keep contaminants and water out of the hydrocarbon stream, and prevent hydrocarbons from leaching into the groundwater.
Cement Hydration	The chemical reaction between cement and water.
Equivalent Circulating Density (ECD)	The effective density of a circulating fluid in the wellbore resulting from the sum of the hydrostatic pressure imposed by the static fluid column and the friction pressure.
Lost Circulation Material (LCM)	The collective term for substances added to wellbore fluids when wellbore fluids are being lost to the formations downhole.
Primary Cementing	The process of mixing a slurry of cement, cement additives, and water and pumping it down through casing to critical points in the annulus around the casing or in the open hole below the casing string.
Pyrolysis	The thermal decomposition of materials at elevated temperatures in an inert atmosphere.
Rheology	The branch of physics that deals with the deformation and flow of matter, especially the non-Newtonian flow of liquids and the plastic flow of solids.

## 1. Introduction

One of the main challenges facing many industries today is the process of decreasing net carbon emissions into the atmosphere. The oil and gas industry is particularly challenged with this dilemma, as many of the processes associated with oil and gas exploration, production, and refining are carbon emission intensive. A specific operation that produces high carbon emissions in the industry is well cementing operations. Cement in oilfield operations has the potential to be an adequate storage mechanism for carbon, since it is permanently installed in the subsurface. The purpose of this study is to investigate novel cement designs that would decrease net carbon emission in oilfield cementing operations by means of carbon sequestration. Three different materials are proposed in this research as possible carbon sequestering additives. These materials are hemp hurd, biochar, and non-recyclable plastic. The goal of this research is to observe the effects the proposed additives have on cement characteristics at various additive rates.

### 1.1. Carbon Emission and Global Warming

In 2020, the reported annual global average carbon dioxide concentration at Earth's surface was  $412.5 \pm 0.1$  parts per million (ppm), which is an increase of  $2.5 \pm 0.1$  ppm compared to 2019 (Blunden & Boyer, 2020). This is the highest carbon dioxide concentration recorded by modern instrumentation and in ice core records dating back 800,000 years. Since 2000, the amount of global atmospheric carbon dioxide has grown by 43.5 ppm, an increase of 12%. This increase in global carbon dioxide levels is believed to be attributed to anthropogenic emissions (Blunden & Boyer, 2020).

Figure 1, created by the National Oceanic and Atmospheric Administration (NOAA), shows the correlation between anthropogenic carbon dioxide emissions and atmospheric carbon dioxide concentrations between 1750 and 2020.

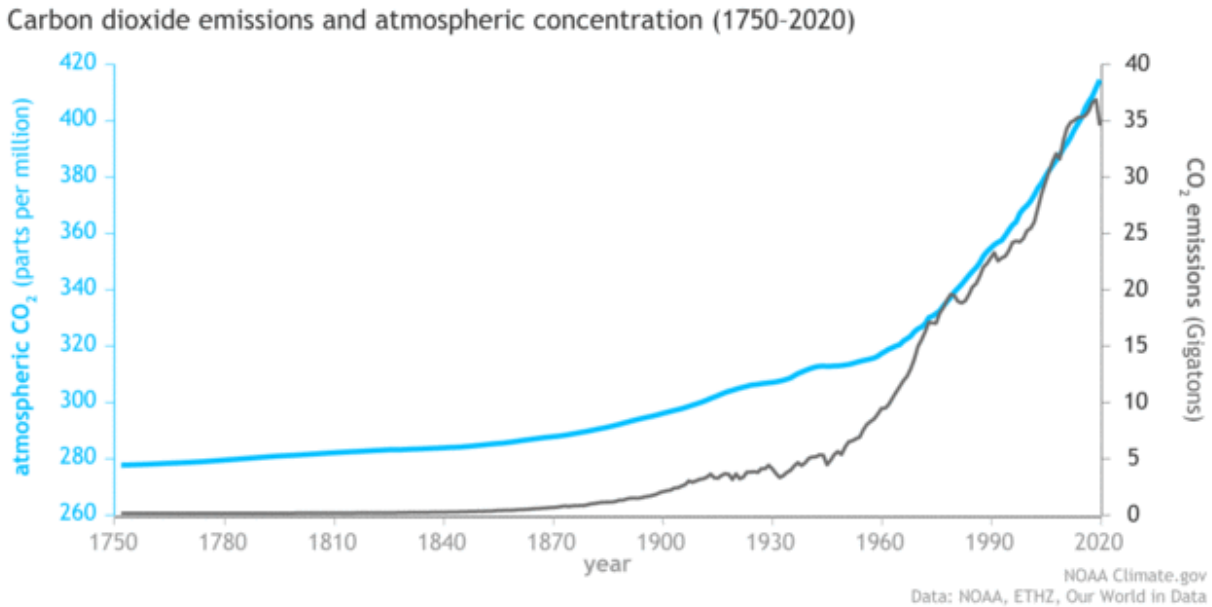


**Figure 1: Carbon dioxide emissions and atmospheric concentration from 1750-2020 (NOAA, 2021)**

### 1.1.1. Global Climate Change

In 1896, a seminal paper by Swedish scientist Svante Arrhenius first predicted that changes in atmospheric carbon dioxide levels could substantially alter surface temperature through the greenhouse effect (Arrhenius, 1896). It is now commonly accepted amongst the scientific community that carbon emission from human activities has an effect on the Earth's temperature (NOAA, 2021). The exact extent of the effects of human-produced carbon emissions on the planet's surface temperature is currently debated among scientists (NOAA, 2021).



## **1.2. Carbon Emission Reduction Investments in the Oil and Gas Industry**

While the extent of the effects of carbon emission on global warming is still debated among scientists, many private corporations are already investing heavily in reducing their carbon emissions. The US oil and gas industry is currently at the forefront of industrial carbon emission reduction investment. Exxon Mobil, the largest U.S.-based oil and gas company, announced in 2021 a plan to invest more than \$15 billion on lower greenhouse gas emission initiatives. This trend is seen throughout most of the industry. Chevron announced in 2021 a commitment to investing more than \$10 billion by 2028 to lower the carbon intensity of their operations. BP announced a plan to reduce net emissions 20% by 2025, 30-35% by 2030, and to be net zero in carbon emissions by 2050. From investments committed by some of the largest oil and gas companies, it is clear that the industry is determined to lower carbon emissions produced through their operations.

## **1.3. Carbon Emissions Associated with Cement Production**

The production of cement is currently the largest single industrial emitter of carbon dioxide into the atmosphere (Ellis et al., 2020). Carbon emissions associated with the production of cement account for approximately 8% of global industrial carbon dioxide emissions. Two factors are the main contributors to this large emission of carbon dioxide from the production of cement. The first of these factors is the creation of carbon dioxide from the decomposition of calcium carbonate ( $\text{CaCO}_3$ ) to calcium oxide ( $\text{CaO}$ ) in the cement manufacturing process. The second main factor is the combustion of fossil fuels (primarily coal) in the calcining and sintering processes in cement production. Around 3.9 billion tons of Ordinary Portland Cement are produced annually, which emits up to 1,244 pounds of carbon dioxide for every ton produced (Ellis et al., 2020).

## 1.4. Cement in the Oil and Gas Industry

Cement is used primarily in two oil and gas industry applications, both of which are associated with the wells used in the industry to access the subsurface hydrocarbon-bearing reservoirs. The first application is well cementing in the completion stage of well construction, also known as primary cementing. In this operation, cement is pumped in the void between the installed steel casing and the borehole. The cement is used to support the casing and protect it from corrosion. The cement also isolates different geological zones of the well from each other, which prevents subsurface fluids (oil, natural gas, or water) from communicating with other geologic zones. Figure 2 illustrates this process of primary well cementing.

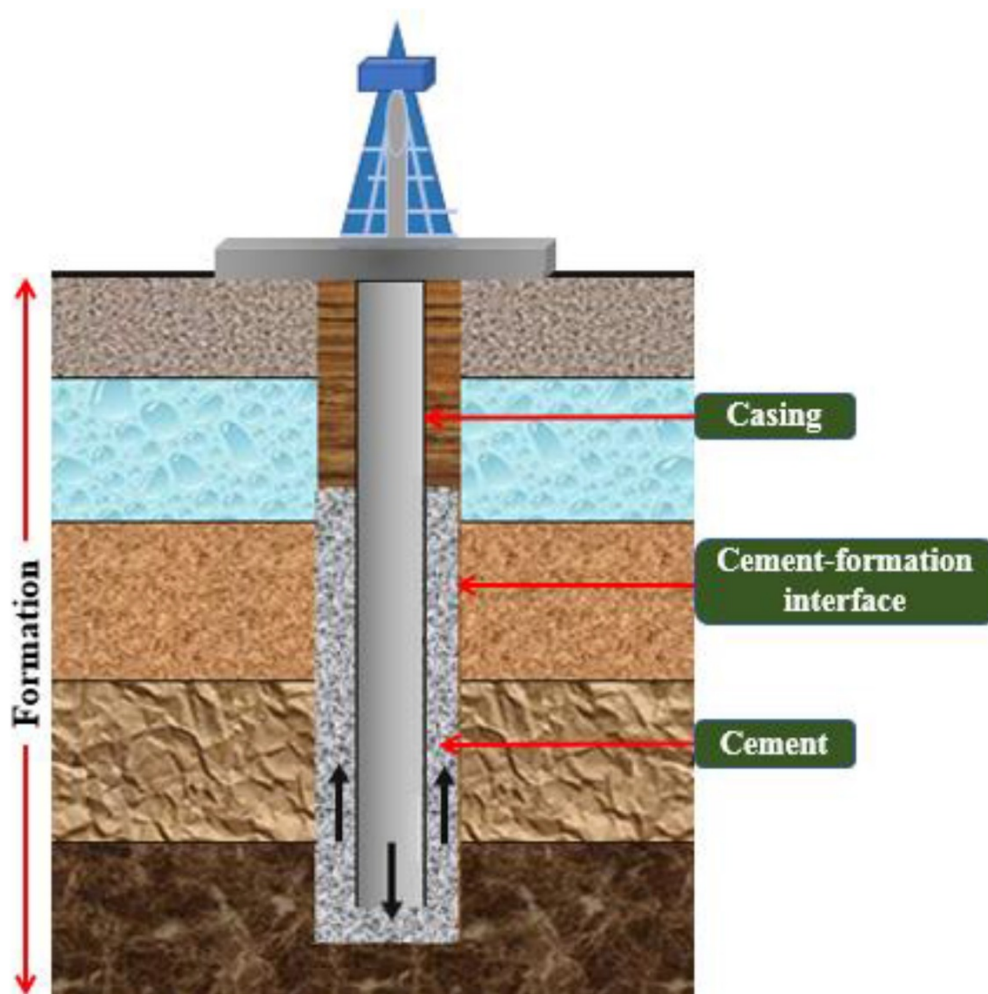


Figure 2: Schematic diagram for primary oil well cementing (Mtaki et al., 2020)

The other main use of cement in the oil and gas industry is in Plug and Abandonment (P&A) operations. P&A operations are conducted to seal in a well that is no longer of use to an operator and to restore the surface location to its original conditions. Cement is used in this operation to seal the well to prevent subsurface fluids from reaching other zones or the surface of the earth. An example of a P&A operation design in an offshore well is displayed in Figure 3. This figure shows the use of cement as a plug to create a reservoir barrier, flow zone barrier, and environmental barrier.

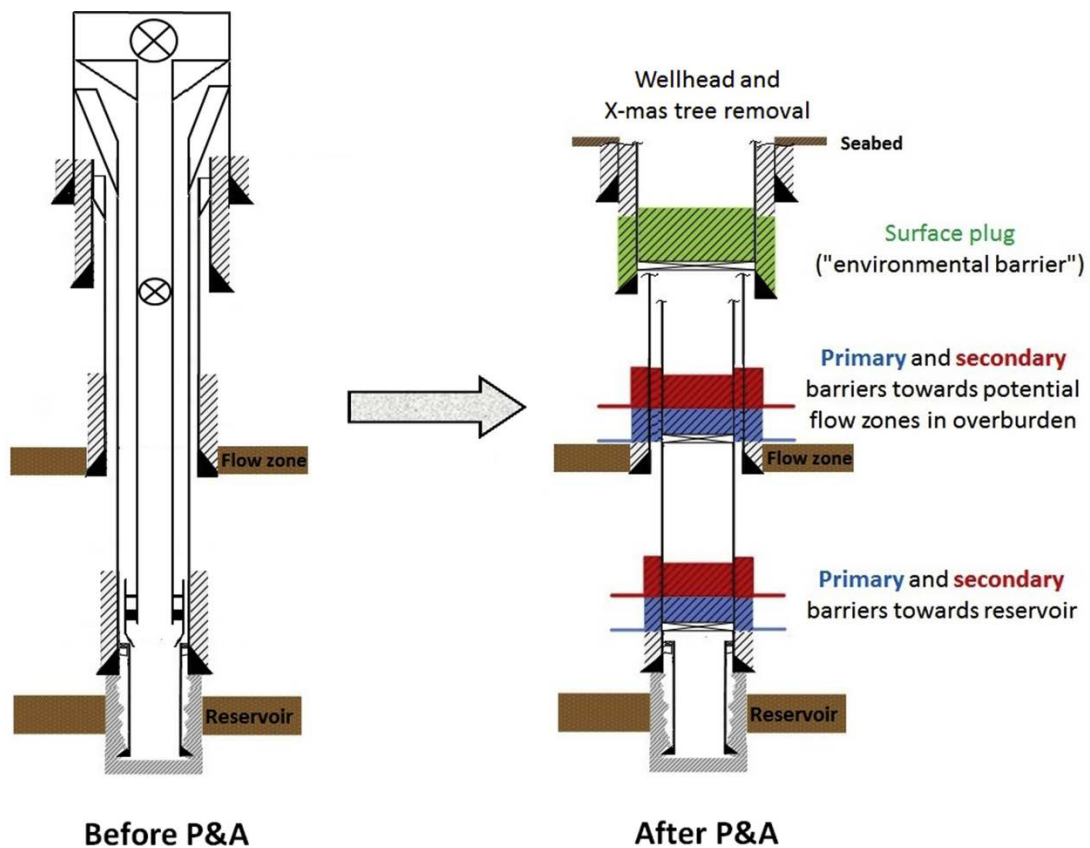


Figure 3: Simplified illustration of a typical offshore production well before and after P&A (Vrålsta et al., 2019)

## 1.5. Carbon Sequestration

According to U.S. Geological Survey (USGS), carbon sequestration is defined as the process of capturing and storing atmospheric carbon dioxide. Carbon Sequestration is typically split into two categories. These categories are geologic carbon sequestration and biologic carbon

sequestration. Geologic carbon sequestration is the process of storing atmospheric carbon dioxide in subsurface geologic formations. Biologic carbon sequestration is the process of storing atmospheric carbon dioxide in vegetation, soils, woody products, and aquatic environments. This is achieved by plant photosynthesis which captures carbon dioxide from the atmosphere and stores it in the materials described previously.

The use of hemp hurd and biochar as oilfield cement additives in this project incorporates both geologic and biologic carbon sequestration methods. Both materials are composed of carbon captured from atmospheric carbon dioxide as a result of plant photosynthesis. This carbon is then stored in subsurface geologic formations by the cement in the oilfield application.

## **1.6. Hemp Hurd**

Hemp hurd (also called shives) is composed of the woody inner layers of a hemp plant stalk. Hemp hurd is collected as a byproduct of hemp fiber processing. Hemp hurd is composed of 44.0% alpha-cellulose, 25.0% hemicellulose, and 23.0% lignin as its major components, along with 4.0% extractives (oil, proteins, amino acids, pectin) and 1.2% ash (Gandolfi et al., 2013).

Hemp hurd was considered to be a waste product of hemp fiber manufacturing, but recently several uses have been found for the byproduct. This can be attributed to the material being considered an eco-friendly substitute for similar less eco-friendly materials. For example, one way hemp hurd is put to use is as an animal bedding material. Another use of hemp hurd is as a main component of a concrete called hempcrete. This hempcrete can be used in several different applications as a substitute for traditional surface building concrete.

## 1.7. Biochar

Biochar is defined as a high carbon content organic material that is created through a process called pyrolysis. The pyrolysis process to create biochar is a thermochemical decomposition of biomass with a temperature of approximately  $\leq 700^{\circ}\text{C}$  in either the absence of or in a limited supply of oxygen (Jamaludin & Tan, 2019). Biochar is primarily composed of carbon (~85%) and can also contain oxygen and hydrogen along with some inorganic ash if it is present in the original biomass (Basu, 2018). Several different types of waste biomass are commonly used to produce biochar. These waste biomasses include livestock manures, sewage sludge, municipal solid waste, paper mill waste, food processing waste, forestry waste, and crop residues (Cantrell et al., 2012; Ahmad et al., 2014). The main use of biochar in industrial applications is as a soil remediation material. Biochar has been researched extensively in recent years in building applications due to its efficiency in sequestering carbon (Legan et al., 2022).

## 1.8. Non-Recyclable Plastics

Plastic is one of the biggest innovations of the 20<sup>th</sup> century and is a material used in almost all aspects of modern life. The growth in popularity of plastic use in all aspects of society has contributed to the production of large amounts of plastic waste in recent times. 6.5 billion tons of plastic waste and discarded rubber are generated every year globally. This waste poses a large ecological threat due to the long degradation period of plastic (Li et al., 2020). Non-recyclable plastics are plastic materials that cannot be recycled with common recycling practices. This inability for these materials to be recycled by conventional means is typically associated with the material's inability to be fed into various machinery in the recycling process or because of how the plastic was created. Plastics can be difficult to run through recycling machinery usually due to the material being too soft or too light. If the plastic is a thermoset plastic, it

contains polymers that form irreversible chemical bonds and cannot be recycled. Some common plastic items that are considered to be non-recyclable include plastic straws, plastic beverage pack rings (eg: six pack rings), bioplastics, and plastic cling film. These materials are largely disposed of since they cannot be recycled conventionally. The typical disposal method of this material is either storage in a landfill or incineration, both of which have negative effects on the environment. Degradation of plastics in landfills leads to the presence of microplastics, which can disseminate into adjacent environments through runoff and leakage and present various environmental hazards (Rahman et al., 2023). The incineration of plastic produces multiple greenhouse gas emissions into the atmosphere, and also has emissions associated with the accelerant used for incineration (Anshassi et al., 2021). For the purpose of this research, non-recyclable plastic carbon sequestration will be quantified by the amount of carbon emission equivalent that is sequestered in the mass of plastic by storing the material underground compared to the material being incinerated.

## **2. Literature Review**

Hemp hurd, biochar, and non-recyclable plastics have been studied as additives in various surface building materials. These materials have yet to be studied as cement additives in oil and gas industry applications. The following sections will elaborate on this opportunity to apply the proposed materials as carbon sequestering additives in oilfield cementing operations.

### **2.1. Hemp Hurd as a Concrete Additive**

The most widely applied use of hemp hurd in recent times is its use as a bio aggregate to make hempcrete. Research has found that hemp concrete behaves differently compared with other traditional building materials. The main advantages found in the material's characteristics as a concrete aggregate are that it has a negative carbon footprint, low density, low thermal conductivity, good moisture buffer capability, and acoustic insulation capabilities (Jami et al., 2019).

The main disadvantage of hempcrete is its relatively low compressive strength. Commercial hemp lime wall systems tend to achieved a compressive strength of approximately 15-30 psi (Sutton et al., 2011), which is only about 5% of the compressive strength of concrete blocks. Compressive strengths were found to increase when cement is added to the design.

Unlike most concrete aggregates that utilize Portland cement as a binder, the majority of hemp hurd concretes have been constructed using a lime binder. Lime-based binder is selected because of its abundance and its low emissions associated with manufacturing. Lime binders are also more compatible with hemp hurd than traditional cement since they aid in preventing the setting of the inner layers of the hemp-cement composite (Walker, 2013).

While hemp hurd has been researched extensively as an aggregate in composites, it is not a good comparison to oilfield cement designs. Typical hempcrete designs utilize a 1:1 aggregate to

binder volumetric ratio. Since hemp hurd is proposed as an additive to oilfield cement, which is designed to consist primarily of Portland cement, the hemp would only constitute a fraction of the volume of Portland cement used in the design. This is also attributed to the fact that aggregate is not utilized in typical oilfield cementing, so the results of hempcrete research cannot be accurately applied to oilfield cement designs. This research aims to discover the effects of hemp hurd on cement designs relating to oilfield cementing operations.

## **2.2. Biochar as a Concrete Additive**

Numerous studies have been done observing biochar as a concrete additive for building materials. Biochar presents a significant carbon footprint reduction potential when used in building materials. From all studies conducted, the dosage of biochar ranged from 0.5% to 40% by weight of the various composites created (Legan et al., 2022). Research shows that in concrete composites with biochar contents up to 24%, compressive strength increased by 12-35% (Gupta et al., 2017, 2018b; Gupta and Kashani, 2021; Qin et al., 2021; Restuccia and Ferro, 2016; Zeidabadi et al., 2018), flexural strength increased by 11-26% (Das et al., 2015; Gupta et al., 2017; Jeon et al., 2021; Praneeth et al., 2021; Restuccia and Ferro, 2016; Suarez-Riera et al., 2020), and tensile strength increased by 3-50% (Gupta et al., 2018b; Qin et al., 2021; Restuccia and Ferro, 2016; Zeidabadi et al., 2018).

Accelerated cement hydration was reported as the primary cause of increased strength in composites after the addition of the biochar additive (Gupta et al., 2018a; Gupta and Kashani, 2021; Qin et al., 2021).

The results found in previous research suggest that not only could biochar sequester carbon in oilfield cementing applications, but it might also improve mechanical properties of the cement. Similar to the studies of hemp hurd as a concrete additive, the research conducted using



biochar as a building material additive was only done on surface concrete structure designs. Consequently, these findings cannot be directly applied to oilfield cement designs, which indicates the need for the proposed research to determine whether the additive can be applied to oilfield cement designs.

### **2.3. Recycled Plastic as a Concrete Additive**

Different forms of recycled plastic have been proposed as possible concrete aggregate replacements to create more environmentally friendly concretes. In one study, fine aggregate was replaced by polyethylene (PE) and poly-ethylene terephthalate (PET) in a lightweight concrete design (Tayeh et al., 2021). PE is the type of plastic found in plastic bottles and PET is the type of plastic typically used in plastic tanks. Figure 4 shows the process from which the PE and PET aggregates were obtained for the study. Five concrete samples containing PE and PET were prepared as partial replacement of the fine aggregate in the design at substitution levels of 0%, 10%, 20%, 30%, and 40% (Tayeh et al., 2021).



**Figure 4: Recycling process of PE and PET wastes (Tayeh et al., 2021)**

The results of the study showed the effects of the PE and PET additives on the mechanical properties of the concrete samples (Tayeh et al., 2021). The study found that concrete density was decreased slightly with the substitution of plastic aggregates into the design. When PE was used as a substitute aggregate at a rate of 20% and 40%, compressive strength decreased by 33.65% and 52.46% respectively after a 28-day curing period. When PET was used as a substitute aggregate at a rate of 20% and 40%, compressive strength decreased by 15.40% and 21.41% respectively after a 28-day curing period. This indicates that PE had a more negative effect on compressive strength compared with PET. Flexural strength was also decreased when both PE and PET aggregates were used at increasing rates (Tayeh et al., 2021).

In a similar study, various shapes of recycled plastic aggregates (RPAs) were studied for mechanical and thermal properties (Basha et al., 2020). The recycled plastic used for this study was collected from a local plastic recycling plant. The plastic aggregate material consisted

mostly of PE and was produced in various shapes including granules, fibers, and flakes. Figure 5 shows the different plastic aggregate shapes used in the study (Basha et al., 2020).

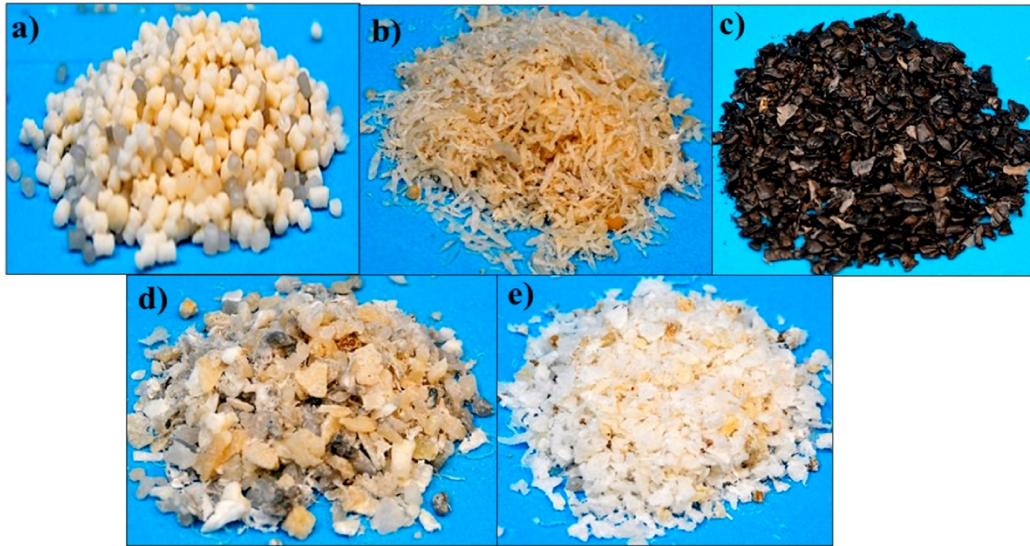


**Figure 5: Types of Recycled Plastic Additive used as replacement of natural coarse aggregates: (a) Granules, (b) Fibers, (c) Black flakes, (d) Mixed flakes, and (e) White Flakes. (Basha et al., 2020)**

The results of the study showed the effects the different recycled plastic additives had on the mechanical and thermal properties of the concrete samples (Basha et al., 2020). Concrete sample density decreased with an increased quantity of RPA. Compressive strength, flexural strength, modulus of elasticity, and bond strength all decreased with increasing amounts of RPA. The RPA shape had an effect of several of these properties. Granule RPA generated a higher compressive strength than fiber and flake RPA. Flake RPA generated a better flexural strength in the concrete samples compared to the granule and fiber RPA. The thermal conductivity of concrete decreased as the amount of RPA was increased in the study. Concrete samples with various concentrations of RPA had a thermal conductivity 35-65% lower than the control concrete. This indicates that concrete with RPA can be utilized as an efficient thermal insulation material (Basha et al., 2020).

Recycled plastic has been studied and proven as a useable aggregate replacement in certain surface structure concrete designs to act as an effective means of disposing waste plastic. Similar to the hemp hurd and biochar concrete additive studies, waste plastic concrete additive studies have only researched the material as a surface construction concrete additive. This material has not yet been studied as a cement additive in an oilfield cementing application. This research aims to fill this gap of knowledge and allow for the characteristics of this additive in an oilfield cement design to be observed.

### **3. Materials and Methods**

To identify the effects of the selected carbon-storing materials on oilfield cement designs, lab experimentation was required for this study. The following sections describe the experimental approach of the study, the materials utilized, and the methods used to acquire experimental data.

#### **3.1. Experimental Approach**

##### **3.1.1. Overview**

Hemp Hurd, Biochar, and Non-Recyclable Plastics were selected as the carbon-storing materials for this study. To begin observing the effects of these materials in an oilfield cement setting, a base cement design was required to build altered designs from. The following section details the base cement design selected for this study. The modifications made to the base cement design to incorporate the novel additives are described in section 3.1.3. A control set of experiments was required to isolate variables for proper data interpretation. The outline and design of these control experiments are described in section 3.1.4.

The primary cement characteristic studied in this research was the unconfined compressive strength of the cement designs and how introduction of the three novel additives affected this characteristic. This was selected as the main characteristic of interest for the study due to the importance of early cement strength development in oilfield cementing operations. Many operations in the oil and gas industry involving cement require the cement design to obtain high strength in a timely manner. For example, during drilling operations cement must reach a desired strength before drilling can resume. Similarly, in well plug and abandonment operations cement must set and reach a desired strength before additional operations can be performed. The early strength of oilfield cement is critical for efficient operations.

To observe the effects of the novel additives on early compressive strength, cement samples were constructed and tested for unconfined compressive strength at various additive rates of the three novel materials. The samples were cured for 12 hours prior to testing in a  $70^{\circ}\text{F} \pm 5^{\circ}\text{F}$  water bath. Additional details on the samples, additive rates, and experimental procedures are presented in the “Materials and Methods” section of this document.

The second primary cement characteristic of interest for this study is the effect of the novel materials on the cement design’s rheological properties. Unlike other industrial applications of cement, in the oil and gas industry cement must be pumped thousands of feet to reach its intended location in the subsurface. In most instances, the cement must be pumped down a string into the subsurface and back up the wellbore through the annulus created by the string and the surrounding geologic formation or previous casing string. The cement pumps must produce enough energy to overcome viscous effects while pumping down the string and up the annulus. This often adds up to high horsepower requirements to complete these cementing operations. Due to the cement slurry rheology’s effect on pumpability, this characteristic is important in determining if the additives are applicable to oilfield cementing operations. In addition, the increase in pump pressure required to circulate higher viscosity cement slurries also has the effect of increasing downhole pressures resulting in high equivalent circulating densities (ECDs). If the cementing operation is executed in a subsurface location where a geologic formation is exposed, the geologic formation will experience this higher downhole pressure. This could be very problematic to the operation if the geologic formation present is too weak to contain this elevated downhole pressure. If this were to occur, the pumped fluid could fracture the formation and wellbore fluids would leak off into the formation, causing difficulties in the cementing operation and potential high cost remediation operations. The potential increases in

pumping horsepower requirements and formation damage risks associated with cement slurry rheology makes the effects of the novel additives' introduction into the cement design important knowledge to understand when considering these carbon-storing materials as oilfield cement additives.

To observe the rheological effects of the three novel cement additives on a cement slurry, sample slurries were constructed and tested for rheological properties at various additive concentrations for the three studied materials. Additional details on the samples, additive rates, and procedures for this process are included in the "Materials and Methods" section of this document.

### **3.1.2. Base Cement Design**

A base cement design was required for this study. The base cement design was then modified to incorporate differing concentrations of the novel carbon-storing materials. Observations were made to identify their effects on an oilfield cement design. To reduce the number of variables affecting the cement's characteristics, a simple low-additive design was selected. This is advantageous in analyzing the effects of the novel additives during testing. The base cement design selected for this study is a common bottom plug cement design utilized for well plug and abandonment operations. The base case cement design is presented in Table 1. The dry cement used in the design was a Portland Limestone Cement sourced from the GCC Trident Plant in Three Forks, Montana. Calcium Chloride mini-pellets were used in the design at an additive rate of 3% by mass. This functions in the design as an accelerator, which allows the thickening time of the cement to decrease. The base case cement design also implements a 0.25 lbs./sack celloflake additive. This additive acts as a Lost Circulation Material (LCM). LCM is used in oilfield cementing operations to prevent the loss of cement to permeable formations and

natural fractures in the subsurface. LCM achieves this by creating an impermeable layer between the loss zone and the wellbore. The last ingredient used in the base cement design was freshwater at an additive rate of 5.0 gal./sack. The calculated slurry density of this cement design is 15.8 pounds per gallon (lbs./gal.) (118.2 lbs./ft.<sup>3</sup>).

**Table 1 - Base Cement Design**

<b>Base Cement Design</b>	
<b>Additive</b>	<b>Additive Amount</b>
Trident IL(10) Portland Limestone Cement	Base Component
Calcium Chloride Mini-Pellets	3%
Celloflake	0.25 lbs./sack
Freshwater	5.0 gal./sack
Calculated slurry density of design = 15.8 lbs./gal. (118.2 lbs./ft <sup>3</sup> )	

### **3.1.3. Modified Cement Design**

Once the base cement design was established for the study, the design was then modified to incorporate the addition of the novel oilfield cement additives. The cement type, calcium chloride additive rate, and water additive rate all remained identical to the base cement design. The modified cement design substitutes the celloflake LCM additive with the novel cement additives. The modified cement design was then further modified by varying the amount of novel additive in each design. Table 2 displays the modified cement design.



**Table 2 - Modified Cement Design**  
**Modified Cement Design**

<b>Additive</b>	<b>Additive Amount</b>
Trident IL(10) Portland Limestone Cement	Base Component
Calcium Chloride Mini-Pellets	3%
Novel Cement Additive	X* lbs./sack
Freshwater	5.0 gal./sack
Cement slurry density varies in relation to X.	
*additive rates ranging from 0.25 lbs./sack to 10.0 lbs./sack	

Slurries created for unconfined compressive strength and rheological testing of the Hemp Hurd additive were created using the modified cement design at ten different additive concentrations. The additive rates utilized were as follows: 0.25 lbs./sack, 0.50 lbs./sack, 1.0 lbs./sack, 1.5 lbs./sack, 2.0 lbs./sack, 2.5 lbs./sack, 3.0 lbs./sack, 4.0 lbs./sack, 5.0 lbs./sack, and 6.0 lbs./sack.

Slurries created for unconfined compressive strength and rheological testing of the Biochar additive were created using the modified cement design at fourteen different additive concentrations. The additive rates utilized were as follows: 0.25 lbs./sack, 0.50 lbs./sack, 1.0 lbs./sack, 1.5 lbs./sack, 2.0 lbs./sack, 2.5 lbs./sack, 3.0 lbs./sack, 4.0 lbs./sack, 5.0 lbs./sack, 6.0 lbs./sack, 7.0 lbs./sack, 8.0 lbs./sack, 9.0 lbs./sack, and 10.0 lbs./sack. The range of additive rates created for the Biochar additive are higher than the other two novel additives due to its ease of mixing at higher additive rates compared with the other novel additives.

Slurries created for unconfined compressive strength and rheological testing of the non-recyclable plastic additive were created using the modified cement design at ten different additive concentrations. The additive rates utilized were as follows: 0.25 lbs./sack, 0.50 lbs./sack, 1.0 lbs./sack, 1.5 lbs./sack, 2.0 lbs./sack, 2.5 lbs./sack, 3.0 lbs./sack, 4.0 lbs./sack, 5.0 lbs./sack, and 6.0 lbs./sack.

### 3.1.4. Establishing a Control

Upon initial experimentation it was discovered that at varying amounts of novel additive, the cement slurry density was measurably affected by the addition of the novel materials. To adequately compare the effects of the novel additives, slurry density needed to be accounted for. A set of control experiments was created to properly compare the effects of the novel cement additive on cement compressive strength while considering slurry density changes. This was achieved by altering the base cement design. The control cement design is displayed in Table 3. The base cement design was altered by removing the celloflake additive and adjusting the mix water rate to achieved the desired cement slurry density.

**Table 3 - Control Cement Design**  
**Control Cement Design**

<b>Additive</b>	<b>Additive Amount</b>
Trident IL(10) Portland Limestone Cement	Base Component
Calcium Chloride Mini-Pellets	3%
Freshwater	X* gal./sack
Cement slurry density varies in relation to X.	
*Freshwater additive rate varied to achieve desired slurry density.	

Ten control designs were established to encompass the range of measured densities observed during the novel additive experiments. These control designs created a range of measured slurry densities between 14.3 and 16.1 lbs./gal. (107.0 lbs./ft.<sup>3</sup> and 120.4 lbs./ft.<sup>3</sup>). With the establishment of these controls, samples were created and tested using the ten control designs to test for unconfined compressive strength and rheological properties. The results of the experiments utilizing these designs were compared with the results of the novel additive experiments.

## **3.2. Materials**

The following sections outline all the materials utilized for experimentation during this study. The base cement components used for the experiments are described in sections 3.2.1, 3.2.2, and 3.2.3. An overview of the specific novel cement additives utilized in the experiments in this study are described in sections 3.2.4, 3.2.5, and 3.2.6.

### **3.2.1. Cement**

The cement utilized for all experimentation in this study was Trident IL(10) Portland Limestone Cement. This cement is produced by the GCC Trident Plant in Three Forks, Montana. Trident IL(10) is a Portland Limestone Cement designed to meet ASTM C595 IL cement with C1157 as High early strength (HE) and Moderate heat of hydration (MS). Trident IL(10) is ground to perform very similarly to type I/II cement. Some of the main advantages of this cement according to the manufacturer are: similar water demand to Ordinary Portland Cement, lower bleeding, improved mechanical properties compared to Ordinary Portland Cement, and less susceptibility to lack of curing.

### 3.2.2. Calcium Chloride Additive

Calcium chloride mini-pellets were used as a cement additive in all cement designs created for this study at an additive rate of 3% by mass of Trident IL(10) Portland Limestone Cement. This functions in the design as an accelerator, which reduces the thickening time of the cement, allowing the cement to set faster. The type of calcium chloride utilized in all experiments was Cal Chlor Corporation 94-97% Calcium Chloride Mini-Pellets. This was selected as the type of calcium chloride to use for the cement designs to match the base case cement design provided for the study. Figure 6 displays the calcium chloride additive pellets used in the study.



**Figure 6 : 94-97% Calcium Chloride Mini-Pellets Picture**

### **3.2.3. Freshwater Additive**

The freshwater additive utilized for all experiments in this study was reverse osmosis water produced in the Montana Technological University Natural Resources Building Lab. Although in the field it is often necessary to source cement build water from various sources that are nearby or otherwise economical, the reverse osmosis water was selected to eliminate any possible effects resultant from changing water chemistry.

### **3.2.4. Hemp Hurd**

The hemp hurd used in the experiments for this study was supplied by IND Hemp in Fort Benton, Montana. IND Hemp supplied two different size grades of hemp hurd material that were collected from screens as a byproduct of hemp fiber processing. These size grades were labelled as “1-20” and 1-16”. The 1-20 hemp hurd is of smaller particle size in comparison to that 1-16 hemp hurd. The two types of hemp hurd are described in the following sections.

#### **3.2.4.1. 1-20 Hemp Hurd**

One of the two hemp hurds utilized in experimentation for this study was 1-20 hemp hurd. This hemp hurd can be generally characterized as a fine sized, dry, almost sawdust-like material. Figure 7 displays the 1-20 hemp hurd used for this study.



**Figure 7: Picture of 1-20 Hemp Hurd Material**

The 1-20 hemp hurd has a measured bulk density of 0.159 grams/mL (1.33 lbs./gal.). This material was sieved to determine particle size distribution (see section 3.3.1 for additive size distribution quantification procedure). Table 4 displays the particle size distribution for the 1-20 hemp hurd material. The material had 0.14% of particles by mass categorized as 5/12 mesh and 9.31% categorized as 12/18 mesh. The majority of this material is categorized in the 18/40 mesh size grade at 88.81% by mass. The material had 1.74% of particles by mass with a mesh size smaller than 40 mesh.

Table 4: 1-20 Hemp Hurd Additive Size Distribution

<b>1-20 Hemp Hurd Additive Size Distribution</b>	
<b>Mesh Size</b>	<b>% by Mass</b>
>5 Mesh	0%
5/12 Mesh	0.14%
12/18 Mesh	9.31%
18/40 Mesh	88.81%
<40 Mesh	1.74%

#### **3.2.4.2. 1-16 Hemp Hurd**

The other type of hemp hurd material utilized in experimentation for this study was 1-16 hemp hurd. This hemp hurd can be generally characterized as a coarser sized, dry, almost straw-like material. Figure 8 displays the 1-16 hemp hurd used for this study.



**Figure 8: Picture of 1-16 Hemp Hurd Material**

The 1-16 hemp hurd material has a lower measured bulk density in comparison to the 1-20 hemp hurd material. The 1-16 hemp hurd has a measured bulk density of 0.110 grams/mL (0.91 lbs./gal). This material was also sieved to determine particle size distribution (see section 3.3.1 for additive size distribution quantification procedure). The 1-16 hemp hurd additive has a much higher percentage of larger size particle distribution compared to the 1-20 hemp hurd additive. Table 5 displays the particle size distribution of the 1-16 hemp hurd material. The material had 0.16% of particles by mass categorized as >5 mesh and 16.50% categorized as 5/12 mesh. The majority of the 1-16 hemp hurd material can be categorized under the 12/18 mesh size at 50.58% by mass. The material had 26.27% of particles by mass categorized as 18/40



mesh and 6.49% categorized as <40 mesh. The 1-16 hemp hurd material has a greater distribution of particle sizes in comparison to the 1-20 hemp hurd.

**Table 5: 1-16 Hemp Hurd Additive Size Distribution**

<b>1-16 Hemp Hurd Additive Size Distribution</b>	
<b>Mesh Size</b>	<b>% by Mass</b>
>5 Mesh	0.16%
5/12 Mesh	16.50%
12/18 Mesh	50.58%
18/40 Mesh	26.27%
<40 Mesh	6.49%

### **3.2.5. Biochar**

A single source of biochar was utilized in all experiments for this study. The biochar used in the experiments for this study was Miller Soils Raw Biochar supplied by Miller Soils in Boulder, Colorado. No data was made available by the supplier as to what the feed materials were or at what pressure and temperature the biochar was produced at during the process of pyrolysis. This biochar can be generally characterized as a powdery, damp, charcoal-like material. Figure 9 displays the biochar utilized for the experiments in this study.



**Figure 9: Picture of Biochar Material Used During Experimentation**

The biochar used for experimentation was evaluated for bulk density which measured 0.242 grams/mL (2.02 lbs./gal). This material had a significantly higher bulk density in comparison to the two hemp hurd materials used for this study. This material was sieved to determine particle size distribution (see section 3.3.1.1 for additive size distribution quantification procedure). Table 6 displays the particle size distribution of the biochar material used for this study. The material had 2.08% of particles by mass greater than 5 mesh. The largest percentage of the biochar material is categorized in the 5/12 mesh size grade at a

concentration of 44.12% by mass. A large amount of the biochar is also present in the 12/18 mesh size grade at a concentration of 41.84% by mass. The material had 11.63% of particles by mass categorized as 18/40 mesh and 0.33% less than 40 mesh. The large majority of the biochar material (85.96% by mass) has a particle size that ranges between 5 and 18 mesh.

**Table 6: Biochar Additive Size Distribution**

<b>Biochar Additive Size Distribution</b>	
<b>Mesh Size</b>	<b>% by Mass</b>
>5 Mesh	2.08%
5/12 Mesh	44.12%
12/18 Mesh	41.84%
18/40 Mesh	11.63%
<40 Mesh	0.33%

### **3.2.6. Non-Recyclable Plastic**

A specific item was selected for testing the non-recyclable plastic additive since there are several common items composed of this material. For this study, six pack can holders were selected as the item in which to derive the non-recyclable plastic for experimentation. Due to varying geometry of the plastic in the six pack rings, only the long outside edges of the can holders were used for experimentation. Once these edges were cut, smaller pieces could then be cut out of the acquired edges. Figure 10 displays the type of six pack can holder used for this study, along with lines to show where the rings were initially cut to acquire the edges for additional sizing. The material left over after the edges were removed was discarded and not used in any of the experimentation for this study.

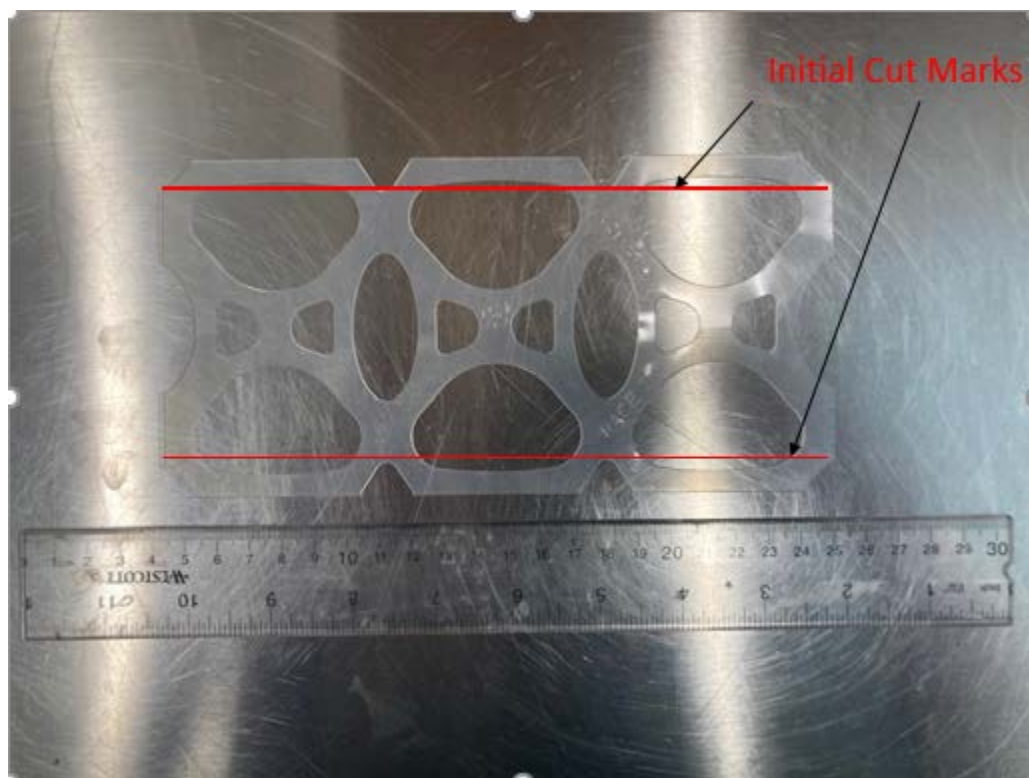


**Figure 10: Diagram of Six Pack can Holder with Initial Cut Marks**

The remaining edges were then cut to form square shaped samples to use as the non-recyclable plastic additive for all experimentation in this study. Figure 11 displays a sample of the material once final cutting was completed. This material's particle size was too large for sieve analysis with the equipment available for the study, so a sample of cut material was measured to acquire the range in size of the material used for experimentation. Side lengths of the square material ranged from 5-10 mm ( $25\text{-}100\text{ mm}^2$  area) with the vast majority of the side lengths remaining within the 6-7 mm ( $36\text{-}49\text{ mm}^2$  area) range. This non-recyclable plastic material has a measured bulk density of 0.253 grams/mL (2.11 lbs./gal). This material had the highest bulk density of the novel additives in this study.



**Figure 11: Picture of Non-Recyclable Plastic Material Used During Experimentation**

### **3.3. Methods**

The following sections describe all of the procedures and testing apparatuses utilized for the experimental portion of this study. All experiments for this research were completed in the Montana Technological University Natural Resources Building Labs. In the following sections, all experimental procedures and equipment are presented for additive particle distribution quantification, preparation of cement slurries, determination of sample slurry densities, determination of cement slurry rheology, creating sample molds for unconfined compressive strength testing, and the testing of samples for unconfined compressive strength.

### **3.3.1. Additive Size Distribution Quantification Using a Sieve**

Sieve analysis was required to better understand the particle size distributions of the three selected novel cement additives. In this study, the two hemp hurd materials and the biochar material were examined for size distribution using a vibrating sieve. Due to mesh size restrictions, the non-recyclable plastic additive was not examined using this method, and was instead examined by manually measuring a sample of the material (see section 3.2.6 for more details).

The apparatus utilized for this process was a Retsch Model AS 200 Vibrating Sieve. The sieve mesh screens selected for this procedure are listed from top to bottom as follows: USA Standard Testing Sieve No. 5 Mesh (4.0 mm), Retsch Sieve No. 12 Mesh (1.7 mm), Retsch Sieve No. 18 Mesh (1.0 mm), and USA Standard Testing Sieve No. 40 Mesh (0.4 mm). A collection tray was also installed in the bottom of the column to collect any materials that passed through the 40 mesh sieve. This apparatus is displayed in Figure 12. All feed materials and materials collected on the sieve screens were massed with an Ohaus Adventure Pro Digital Scale which recorded the mass with precision of 0.01 grams. The following section details the procedure used for quantifying the size distribution of the 1-16 hemp hurd, 1-20 hemp hurd, and biochar additives.



**Figure 12: Retsch Model AS 200 Vibrating Sieve**

### **3.3.1.1. Additive Size Distribution Quantification Procedure**

1. Install the collection tray at the bottom of the Retsch AS 200 Vibrating Sieve, then install the following sieves in order: USA Standard Testing Sieve No. 40 Mesh (0.4 mm), Retsch Sieve No. 18 Mesh (1.0 mm), Retsch Sieve No. 12 Mesh (1.7 mm), and USA Standard Testing Sieve No. 5 Mesh (4.0 mm).
2. Mass out 50.00 grams of the novel cement additive using an Ohaus Adventure Pro Digital Scale and pour the material into the top sieve.
3. Install the lid on the vibrating sieve and begin vibrating the material at an amplitude of 55 for ten minutes.

4. Once the Retsch AS 200 Vibrating Sieve is turned off, remove the lid from the apparatus.
5. Remove the first sieve tray and collect all material contained on the screen.
6. Measure and record the mass of the material collected with a 0.01 gram precision using an Ohaus Adventure Pro Digital Scale.
7. Repeat steps 5 and 6 for each mesh screen in the column.
8. Collect all remaining material in the bottom collection tray and record the mass of the material with a precision of 0.01 grams using an Ohaus Adventure Pro Digital Scale.

### **3.3.2. Preparation of Cement Slurry**

This section presents the equipment and procedures used in this study to create the cement slurries required for density, unconfined compressive strength, and rheological property testing. The procedure for this process is based on American Petroleum Institute (API) recommended practices presented in API RP 10B-2. The cement and water in this procedure were massed with a precision of 0.1 grams using an Ohaus Scout Pro 4000 Gram Digital Scale. The novel cement additives and the calcium chloride additive were massed with a precision of 0.01 grams using an Ohaus Adventure Pro Digital Scale. The cement blender utilized for this procedure was a Waring Commercial Blender. The following section details the procedure utilized in this study for preparing the cement slurries for testing.

#### **3.3.2.1. Preparation of Cement Slurry Procedure (Based on API RP 10B-2)**

1. Measure out required mass of Trident IL(10) Portland cement using an Ohaus Scout Pro Digital Scale with a precision of 0.1 grams.



2. Measure out required mass of calcium chloride additive using an Ohaus Adventure Pro Digital Scale with a precision of 0.01 grams.
3. Measure out required mass of novel cement additive using an Ohaus Adventure Pro Digital Scale with a precision of 0.01 grams.
4. Measure out required mass of reverse osmosis water using an Ohaus Scout Pro Digital Scale with a precision of 0.1 grams.
5. Blend dry materials (Trident IL(10), calcium chloride, and novel cement additive) with a stirring rod.
6. Place measured out amount of water in the Waring Commercial Blender.
7. Turn on blender to the low repetitions per minute (rpm) setting.
8. Add dry cement/additive blend to the blender at a uniform rate in not more than 15 seconds.
9. When all materials have been added to the blender, place the cover on the blender, turn the rotational speed of the blender to the high rpm setting, and continue mixing for 35 seconds.
10. Turn off the blender and remove blender cup from the blender.

### **3.3.3. Determination of Cement Sample Slurry Density Using a Mud Balance**

This section details the equipment and procedure used to determine the fluid density of the cement slurries examined in this study. The procedure for this process is based on American Petroleum Institute (API) recommended practices presented in API RP 10B-2. The apparatus used to measure the cement density in this procedure was a Fann Mud Balance with the capability of expressing fluid density with a precision of 0.1 lbs./gal. The next section details the procedure used to determine cement slurry density for all experiments carried out in this study.

#### **3.3.3.1. Determination of Cement Sample Slurry Density Procedure (Based on API RP 10B-2)**

1. Pour an amount of cement slurry sufficient enough to fill the Fann Mud Balance chamber into the apparatus.
2. Puddle the cement slurry in the mud balance with a puddling rod 25 times to eliminate entrapped air.
3. Install the lid onto the mud balance cup, ensuring that cement slurry leaks out of the top hole.
4. Clean off excess cement that leaks out from the top hole of the mud balance cup.
5. Read and record the slurry density from the mud balance to an accuracy of 0.1 lbs./gal.
6. Dispose of cement sample and clean mud balance.

#### **3.3.4. Determination of Cement Slurry Rheological Properties Using a Rotational Viscometer**

This section details the equipment and procedure utilized in this study to measure the rheology of cement slurry samples. The procedure for this process is based on American Petroleum Institute (API) recommended practices presented in API RP 10B-2. The apparatus used to measure rheological properties of the cement slurries in this study was a Fann Model 35A Rotary Viscometer. This viscometer measures deflection at various shear rates, and from these values viscosity and gel strength data can be calculated. A picture of the Fann Model 35A Rotary Viscometer is shown in Figure 13. The following section describes the procedure used in all experiments in this study to determine cement slurry rheology using the Fann Model 35A Rotary Viscometer.



Figure 13: Picture of a Fann Model 35A Rotary Viscometer

#### 3.3.4.1. Determination of Cement Slurry Rheological Properties Procedure (based on API RP 10B-2)

1. Pour the cement slurry into the viscometer cup to the fill line. Record the initial slurry temperature with a precision of  $0.1^{\circ}\text{F}$ .
2. With the sleeve rotating at the lowest speed, raise the cup until the liquid level is at the inscribed line on the sleeve.
3. Take the initial dial reading 10 seconds after continuous rotation at the lowest speed (3 rpm).
4. Take all remaining readings first in ascending order (6 rpm, 100 rpm, 200 rpm, and 300 rpm), and then in descending order (200 rpm, 100 rpm, 6 rpm, and 3

rpm), after continuous rotation of 10 seconds at each speed. Shifting to the next speed shall be done immediately after taking each reading.

5. Increase viscometer speed to 300 rpm for 10 seconds, then turn the viscometer off for 10 seconds.
6. Set the viscometer at a speed of 3 rpm and start rotation. Record the maximum observed reading immediately after turning on the instrument. This value is used as the 10 second gel strength.
7. Measure and record the final slurry temperature with a precision of 0.1°F.
8. Remove slurry from the viscometer cup and clean viscometer components.

### **3.3.5. Creating Sample Molds for Unconfined Compressive Strength Testing**

This section presents the equipment and procedures utilized in this study to create sample molds for unconfined compressive strength testing. The procedure for this process is based on American Petroleum Institute (API) recommended practices presented in API RP 10B-2. The cement molds selected for this procedure were Humboldt Model H-2820 Brass Cement Molds. Utilization of this mold would produce 3 samples at a time that can be tested for unconfined compressive strength. These samples are cubic in shape and measure 2 inches in height, 2 inches in width, and 2 inches in length. Figure 14 displays a picture of the Humboldt Model H-2820 Brass Cement Mold. After preparation of the cement molds, all samples in the study were cured in a  $70^{\circ}\text{F} \pm 5^{\circ}\text{F}$  water bath for 12 hours prior to testing for unconfined compressive strength. In all experiments, the cement molds were prepared directly after the cement slurry was mixed and slurry density values were measured. The following section describes the procedure used in all experiments in this study to create sample molds for unconfined compressive strength testing.



**Figure 14: Picture of Humboldt Model H-2820 Cement Mold**

**3.3.5.1. Creating Sample Molds for Unconfined compressive Strength Testing Procedure (based on API RP 10B-2)**

1. Lightly coat interior faces of the Humboldt H-2820 Mold and the contact surfaces of the plates with a mold release agent.
2. Pour the cement slurry into the prepared molds to approximately one-half of the mold depth. Puddle each sample approximately 30 times with a puddling rod after all mold chambers have received slurry.
3. Stir the remaining slurry by hand with a stirring rod to suspend the components of the slurry.

4. Fill each sample mold to overflowing with slurry and puddle each sample approximately 30 times with a puddling rod.
5. Strike off the excess slurry even with the top of the mold using a straight edge.
6. Place cover plates on top of molds.
7. Discard any samples in molds that leak.
8. Immediately place molds in a water curing bath set to target curing temperature ( $70^{\circ}\text{F} \pm 5^{\circ}\text{F}$ ).
9. Allow samples to cure for target curing time before testing (12 hours).
10. 45 minutes prior to the end of curing, remove the molds from the water bath and remove the samples from the molds. Immediately immerse the samples in a water bath at approximately  $85^{\circ}\text{F} \pm 5^{\circ}\text{F}$  until the samples are tested.

### **3.3.6. Testing Cement Samples for Unconfined Compressive Strength**

This section details the equipment and procedure utilized to test the cement samples of this study for unconfined compressive strength after a 12-hour curing period. The procedure for this process is based on American Petroleum Institute (API) recommended practices presented in API RP 10B-2. The apparatus used in this study to determine unconfined compressive strength was the Carver Hydraulic Unit Model #3912. This apparatus is displayed in Figure 15. This apparatus is capable of recording maximum pound-force readings with a precision of 100 lbf. All samples in this study were tested for unconfined compressive strength immediately after the 12-hour cure period was reached. The following section describes the procedure used in all experiments in this study to test cement samples for unconfined compressive strength.



**Figure 15: Picture of Carver Hydraulic Unit Model #3912**

**3.3.6.1. Testing Samples for Unconfined Compressive Strength Procedure  
(based on API RP 10B-2)**

1. Place cured cement sample in Carver Hydraulic Unit Model #3912.
2. Load the sample at a rate of 16,000 lbf  $\pm$  1600 lbf per minute.
3. Continue loading the sample until compressive failure.
4. Record the maximum load (within 100 lbf accuracy) on the sample before compressive failure.

5. Report compressive strength as the maximum load divided by the smallest cross-sectional area in contact with the load-bearing plates.

### **3.4. Materials and Methods Conclusion**

The material provided in the “Materials and Methods” section of this work details all of the experimental approaches, materials utilized, and procedures administered to carry out the lab experimentation portion of this study. The base cement design used to develop the novel designs was presented. The modified cement design approach was detailed to explain how base cement design would be manipulated to incorporate the novel materials proposed in this study. A control set of experiments was established so that the effects of the novel materials on the cement design’s characteristics could be analyzed. The base cement design materials used in experimentation were presented, along with the novel cement additives. The novel cement additives used in experimentation were characterized by size distribution and bulk density, along with other physical characteristics observed regarding the materials. The apparatuses and procedures used for the experiments was presented, which included determination of particle size distribution of the novel materials, preparation of the cement slurry, determination of slurry density, determination of cement slurry rheological properties, creation of sample molds for unconfined compressive strength analysis, and the testing of cement samples for unconfined compressive strength.

In the next section, the results of the experiments described in this section will be presented.



## 4. Results

This section presents the results of the experimentation conducted for this study. The first section of this chapter will cover the results of unconfined compressive strength testing of the control cement designs and the novel additive cement designs implementing the use of hemp hurd, biochar, and non-recyclable plastic. Slurry density data will also be provided in this section along with the unconfined compressive strength data.

The second section of this chapter will detail the results of rheological property testing of the control cement designs and the novel additive cement designs. This will include calculated apparent viscosity data and 10 second gel strength data.

Ten designs, implementing both sizes of hemp hurd were created in the lab and tested for slurry density, unconfined compressive strength, and rheological properties. Fourteen cement designs implementing biochar were created in the lab and tested for slurry density, unconfined compressive strength, and rheological properties. Finally, ten cement designs implementing non-recyclable plastic were created in the lab and tested for slurry density, unconfined compressive strength, and rheological properties. The following sections will detail the results of testing related to the 54 cement designs listed above.

### 4.1. Unconfined Compressive Strength Results

This section outlines the results of unconfined compressive strength experimentation in this study. The unconfined compressive strength results in this section are split into four sections. Those sections being the control group, the hemp hurd additive designs, the biochar additive designs, and the non-recyclable plastic additive designs. The control group results will be reintroduced in the novel additive sections to provide a comparison between the results of the control group and the novel additives in relation to slurry density. The measured slurry density

results will also be displayed in this section. Every unconfined compressive strength test was conducted directly after the cement was cured in a  $70^{\circ}\text{F} \pm 5^{\circ}\text{F}$  water bath for 12 hours.

#### **4.1.1. Control Group Unconfined Compressive Strength Results**

This section contains the results of unconfined compressive strength testing of the control group of cement designs in this study. Ten cement designs were established for testing in this control group. The cements were designed to establish a slurry density range of 14.3 to 16.1 lbs./gal. ( $107.0 \text{ lbs./ft.}^3$  to  $120.4 \text{ lbs./ft.}^3$ ). Three cement samples were constructed for each of the ten control designs and tested for unconfined compressive strength after a 12-hour curing period. The results of the unconfined compressive strength testing of the control group are presented in Figure 16. The figure displays the compressive strength values recorded in experimentation in relation to the measured slurry density of the cement.

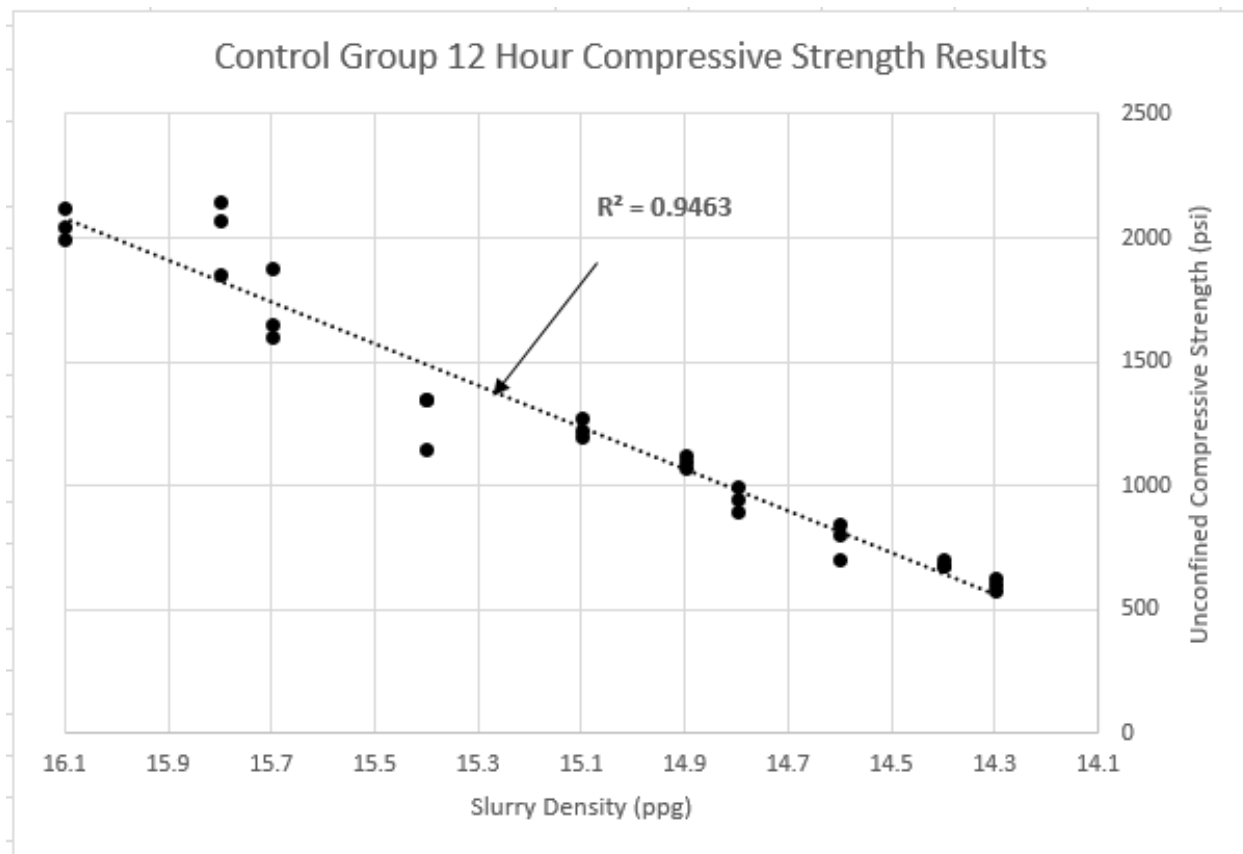


**Figure 16: Control Group 12 Hour Compressive Strength Results**

This comparison shows that as measured cement slurry density decreases for a design, there is a subsequent decrease in the unconfined compressive strength of the material. This is an expected outcome as cement slurry density is typically directly related to the early strength of the cement. The figure also displays a linear trendline created from the data set. This trend has an  $R^2$  value of 0.9463, which indicates the strong linear relationship between slurry density and unconfined compressive strength for the control group. These results create a baseline to compare the effects of the novel cement additives on the cement design.

#### **4.1.2. Hemp Hurd Additive Unconfined Compressive Strength Results**

This section contains the results of unconfined compressive strength testing of the novel hemp hurd additive cement designs in this study. Two separate hemp hurd sizes were tested for

unconfined compressive strength. Ten cement designs incorporating 1-20 hemp hurd were created with the following additive concentrations: 0.25 lbs./sk, 0.5 lbs./sk, 1.0 lbs./sk, 1.5 lbs./sk, 2.0 lbs./sk, 2.5 lbs./sk, 3.0 lbs./sk, 4.0 lbs./sk, 5.0 lbs./sk, and 6.0 lbs./sk. Nine samples were tested for unconfined compressive strength at each of the 1-20 hemp hurd concentrations. The slurry density of each additive concentration was also recorded.

Ten cement designs incorporating 1-16 hemp hurd were created with the following additive concentrations: 0.25 lbs./sk, 0.5 lbs./sk, 1.0 lbs./sk, 1.5 lbs./sk, 2.0 lbs./sk, 2.5 lbs./sk, 3.0 lbs./sk, 4.0 lbs./sk, 5.0 lbs./sk, and 6.0 lbs./sk. Three samples were tested for unconfined compressive strength at each of the 1-16 hemp hurd concentrations. The slurry density of each additive concentration was also recorded.

The results of the unconfined compressive strength analysis of the 1-20 and 1-16 hemp hurd additives are displayed in Figure 17. This figure presents the compressive strength results for the two hemp hurd additives as a function of the additive rate of the cement design. The compressive strength values are plotted as the average values at each additive rate with error bars signifying the range of values obtained during experimentation.

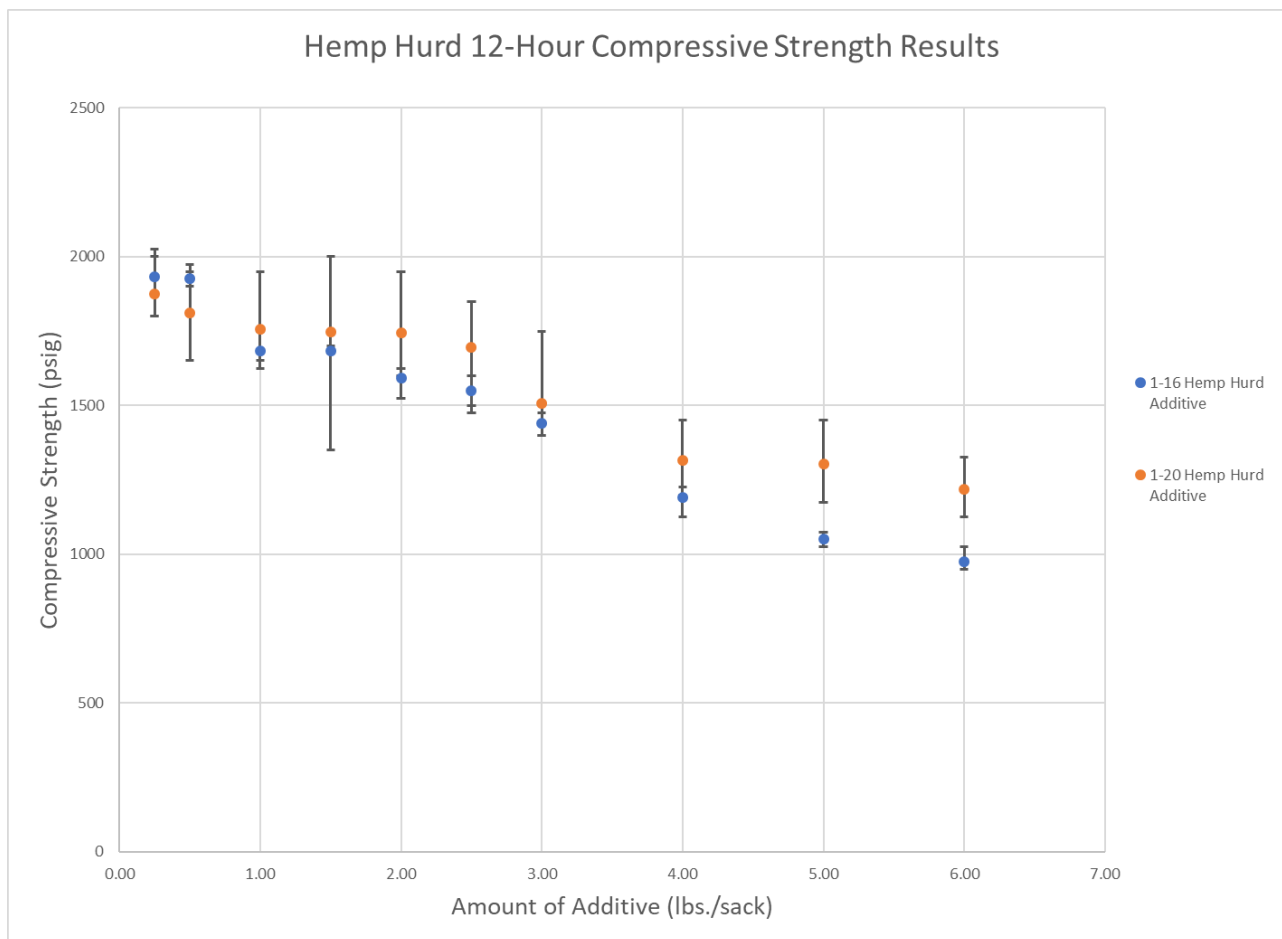


**Figure 17: Hemp Hurd 12-Hour Compressive Strength vs. Additive Rate Chart**

Addition of both hemp hurd additives results in a decrease in unconfined compressive strength with increasing hemp hurd concentration. Both of the hemp hurd additives appear to retain unconfined compressive strength with addition of more additive at lower total additive rates. However, unconfined compressive strength appears to decrease at a much larger rate with the addition of hemp hurd additive at higher total additive rates. The largest decrease in unconfined compressive strength for both hemp hurd additives appears to be between 3.0 lbs./sk and 4.0 lbs./sk. From 0.25 lbs./sk to 2.0 lbs./sk, both hemp hurd additives have similar unconfined compressive strengths. At additive rates above 2.0 lbs./sk, the 1-20 hemp hurd additive has higher unconfined compressive strength values in comparison to the 1-16 hemp hurd

additive. This trend in the data is apparent from the projected linear trendlines of the two materials, in which the unconfined compressive strength difference of the two materials increases with increasing additive rate. This is most likely attributed to the fact that slurry densities are higher in designs implementing 1-20 hemp hurd compared with the slurry densities in designs implementing 1-16 hemp hurd at matching additive rates.

Figure 18 shows the effects of the addition of the hemp hurd additives on unconfined compressive strength in relation to the measured slurry density of the designs. The control group linear data trend is also presented in the figure to be used as a comparison to the designs implementing the novel additives. The compressive strength values are plotted as the average values at each additive rate with error bars signifying the range of values obtained during experimentation.

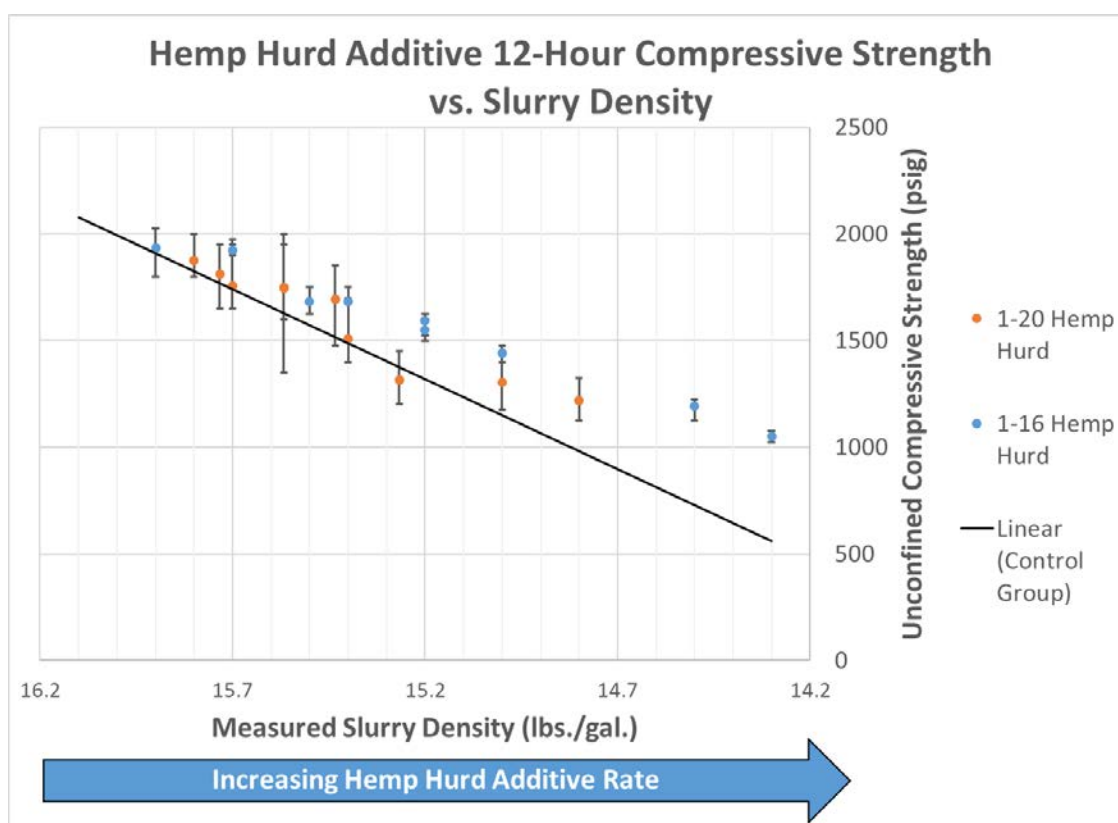


**Figure 18: Hemp Hurd 12 Hour Compressive Strength vs. Slurry Density Chart**

Both grades of hemp hurd additives manifested higher compressive strengths vs the control group across all densities. The 1-16 hemp hurd additions resulted in higher compressive strengths than the 1-20 hemp hurd additions.

#### **4.1.3. Biochar Additive Unconfined Compressive Strength Results**

This section details the results of unconfined compressive strength testing of the novel biochar additive cement designs in this study. For all other additives used in this study, ten cement designs were created and tested at additive rates ranging between 0.25 lbs./sk and 6.0 lbs./sk. This was the initial experimental approach when testing the biochar additive. Upon experimentation of the material in cement designs, it was discovered that the biochar additive had very good mixing properties and higher additive rates could be achieved by this study's lab mixing capabilities using the biochar additive. For this reason, additional biochar additive rate designs were created and tested for unconfined compressive strength. Fourteen cement designs utilizing biochar additive rates ranging from 0.25 lbs./sk to 10.0 lbs./sk were created and examined for unconfined compressive strength. The additive rate used in these tests are as follows: 0.25 lbs./sk, 0.5 lbs./sk, 1.0 lbs./sk, 1.5 lbs./sk, 2.0 lbs./sk, 2.5 lbs./sk, 3.0 lbs./sk, 4.0 lbs./sk, 5.0 lbs./sk, 6.0 lbs./sk, 7.0 lbs./sk, 8.0 lbs./sk, 9.0 lbs./sk, and 10.0 lbs./sk. Three samples were constructed and tested for unconfined compressive strength at each additive rate. The results of the unconfined compressive strength analysis of the biochar additive are displayed in Figure 19, which presents the compressive strength results for the biochar additive as a function of the additive rate of the cement design. The compressive strength values are plotted as the average values at each additive rate with error bars signifying the range of values obtained during experimentation.

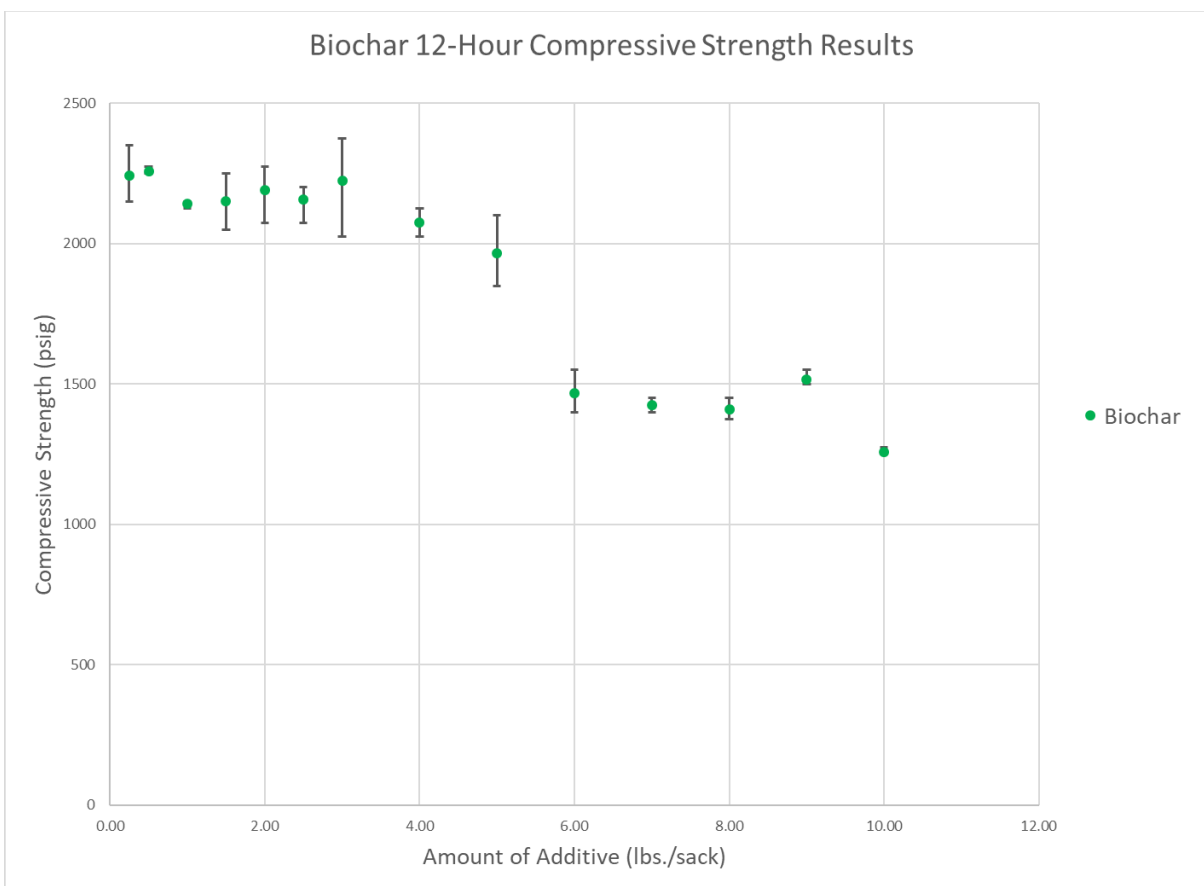


**Figure 19: Biochar 12 Hour Compressive Strength vs. Additive Rate Chart**

Addition of the biochar additive results in a decrease in unconfined compressive strength with increasing amounts of the biochar additive. Unconfined compressive strength appears to be mostly retained in the cement designs utilizing biochar additive rates up to 5.0 lbs./sk. From 5.0 lbs./sk to 6.0 lbs./sk, there is a dramatic decrease in unconfined compressive strength. These lower compressive strength values continue from 6.0 lbs./sk to 10.0 lbs./sk.

Figure 20 is displayed to show the effects of the addition of the biochar additive on unconfined compressive strength in relation to the measured slurry density of the designs. The control group data trendline is also presented in the figure to be used as a comparison to the designs implementing the novel additive. The compressive strength values are plotted as the average



values at each additive rate with error bars signifying the range of values obtained during experimentation.

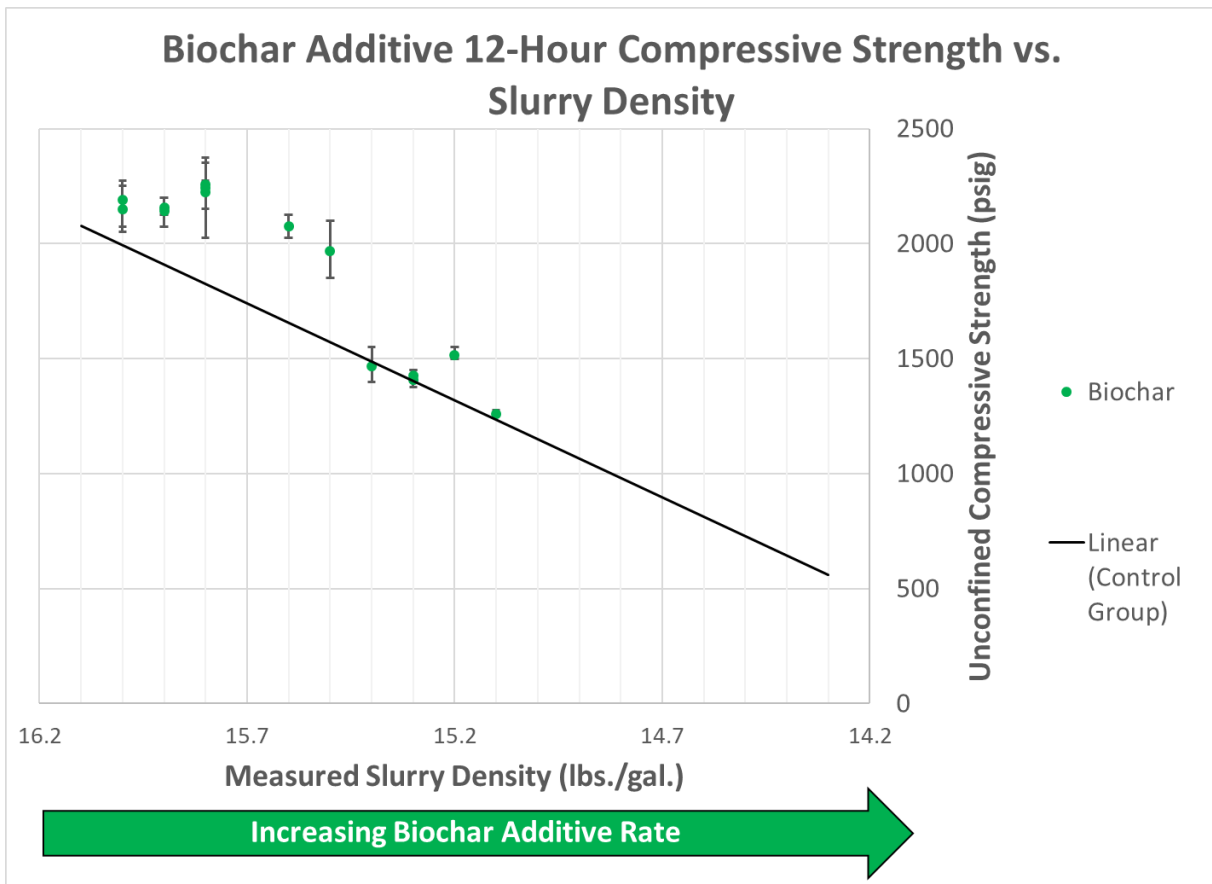


**Figure 20: Biochar 12 Hour Compressive Strength vs. Slurry Density Chart**

The biochar additive designs manifested higher compressive strengths vs the control group at slurry densities between 16.0 lbs./gal. (119.7 lbs./ft.<sup>3</sup>) and 15.4 lbs./gal. (115.2 lbs./ft.<sup>3</sup>). At slurry densities between 15.4 lbs./gal. (115.2 lbs./ft.<sup>3</sup>) and 15.1 lbs./gal. (112.9 lbs./ft.<sup>3</sup>), the biochar additive designs manifested similar compressive strengths to the control group.

#### **4.1.4. Non-Recyclable Plastic Unconfined Compressive Strength Results**

This section contains the results of unconfined compressive strength testing of the novel non-recyclable additive cement designs in this study. Ten cement designs were implemented for testing the novel non-recyclable plastic additive for unconfined compressive strength. The additive rates utilized for these designs are as follows: 0.25 lbs./sk, 0.5 lbs./sk, 1.0 lbs./sk, 1.5 lbs./sk, 2.0 lbs./sk, 2.5 lbs./sk, 3.0 lbs./sk, 4.0 lbs./sk, 5.0 lbs./sk, and 6.0 lbs./sk. Three samples for each additive rate were constructed and tested for unconfined compressive strength after a 12-hour curing period. The results of the unconfined compressive strength analysis of the non-recyclable plastic additive are presented in Figure 21. This figure presents the compressive strength results for the non-recyclable plastic additive as a function of the additive rate of the cement design. The compressive strength values are plotted as the average values at each additive rate with error bars signifying the range of values obtained during experimentation.

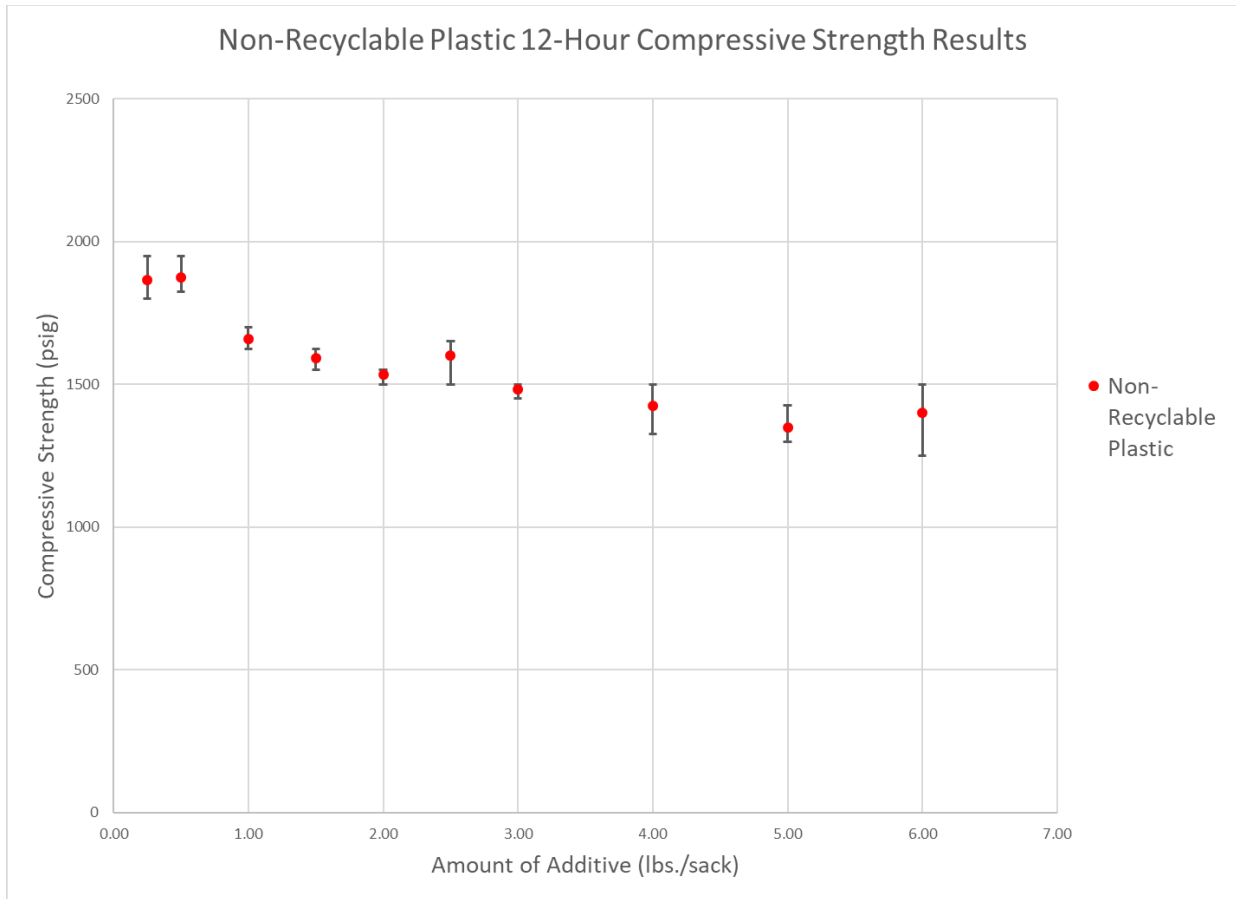


**Figure 21: Non-recyclable Plastic 12 Hour Compressive Strength vs. Additive Rate Chart**

Addition of the non-recyclable plastic additive resulted in a decrease in unconfined compressive strength with increasing amounts of the non-recyclable plastic additive. The decrease in unconfined compressive strength correlates linearly with the increase of additive rate. There does not appear to be any high magnitude abrupt decreases in unconfined compressive strength as observed with the other novel additives.

Figure 22 is presented to show the effects of the addition of the non-recyclable plastic additive on unconfined compressive strength in relation to the measured slurry density of the designs. The control group data is also presented in the figure to be used as a comparison to the designs implementing the novel additive. The compressive strength values are plotted as the

average values at each additive rate with error bars signifying the range of values obtained during experimentation.

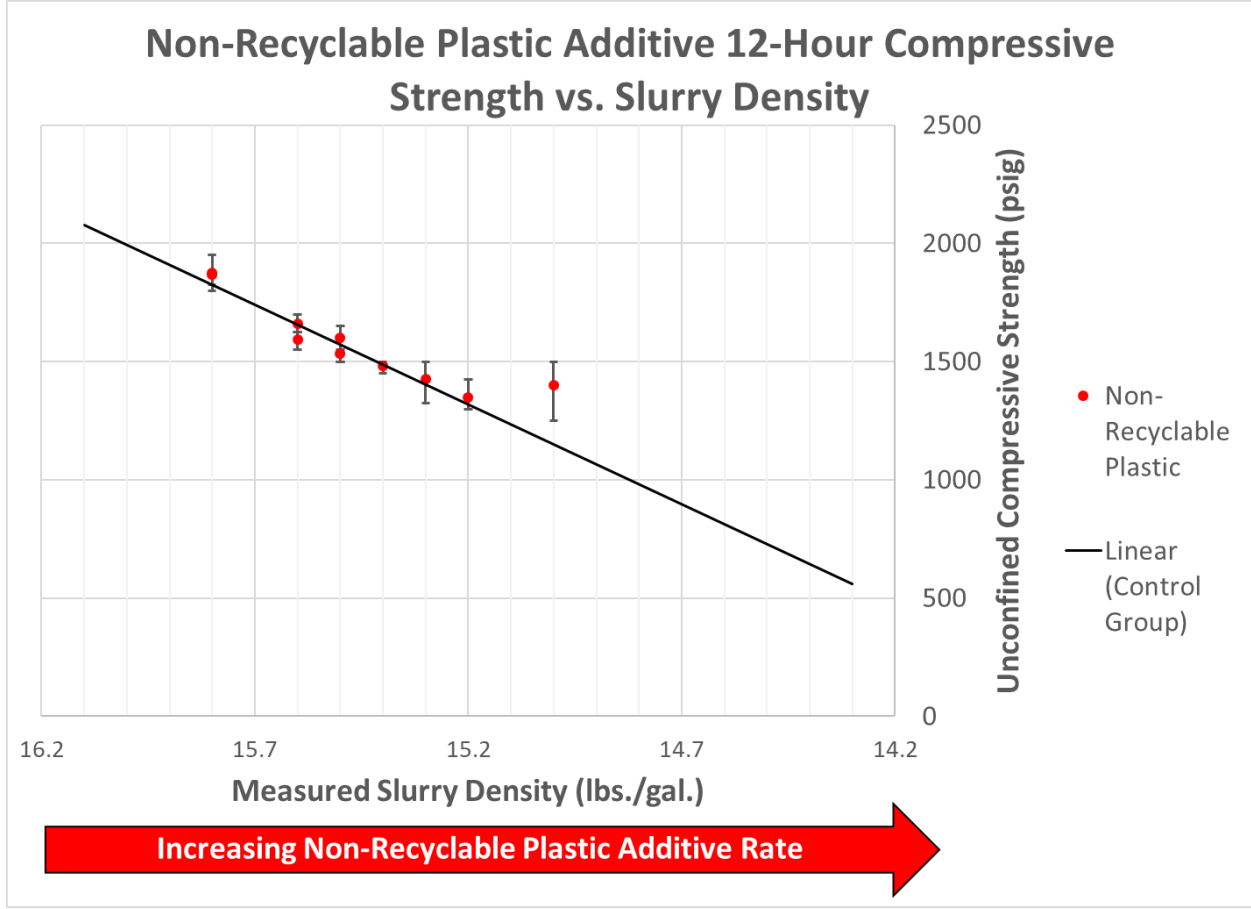


**Figure 22: Non-Recyclable Plastic 12 Hour Compressive Strength vs. Slurry Density Chart**

The unconfined compressive strengths of the designs utilizing non-recyclable plastic additive appear to trend almost identically to the unconfined compressive strengths of the control group at matching cement slurry densities. The unconfined compressive strengths of the designs utilizing non-recyclable plastic additive are very similar to the control group at matching cement slurry densities.

## 4.2. Rheological Testing Results

This section presents the results of rheological testing pertaining to the control group and various additive concentrations of the three novel cement additives investigated in this study. The rheological property results in this section are split into four sections - those section being the control group, the hemp hurd additive designs, the biochar additive designs, and the non-recyclable plastic additive designs. The control group results will be reintroduced in the novel additive sections to provide a comparison between the results of the control group and the novel additives in relation to slurry density. Every rheology test was conducted directly after the cement was mixed. All cement slurries were tested at a slurry temperature of  $95^{\circ}\text{F} \pm 5^{\circ}\text{F}$ .

### 4.2.1. Control Group Rheological Testing Results

This section contains the results of rheological testing of the control group of cement designs in this study. The cements were designed to establish a slurry density range of 14.3 to 16.1 lbs./gal (107.0 lbs./ft<sup>3</sup> to 120.4 lbs./ft<sup>3</sup>). Apparent viscosity is calculated from the dial reading at a preset RPM speed using the following equation:

$$\mu_a = 3000\theta_N / N$$

(1) Apparent  
Viscosity  
Equation

where  $\mu_a$  is apparent viscosity in centipoise (cp),  $\theta_N$  is the dial deflection at the given RPM, and N is the RPM of the rotary viscometer.

Results of apparent viscosity testing of the control group and novel additive designs were all calculated based on a ramp-up speed setting of 100 RPM. This was done to isolate apparent viscosity values at a single RPM speed, which allows the apparent viscosity values for the various additives and rates to be compared effectively. Figure 23 displays the apparent viscosity of the control cement design slurries in relation to the slurry's measured density.

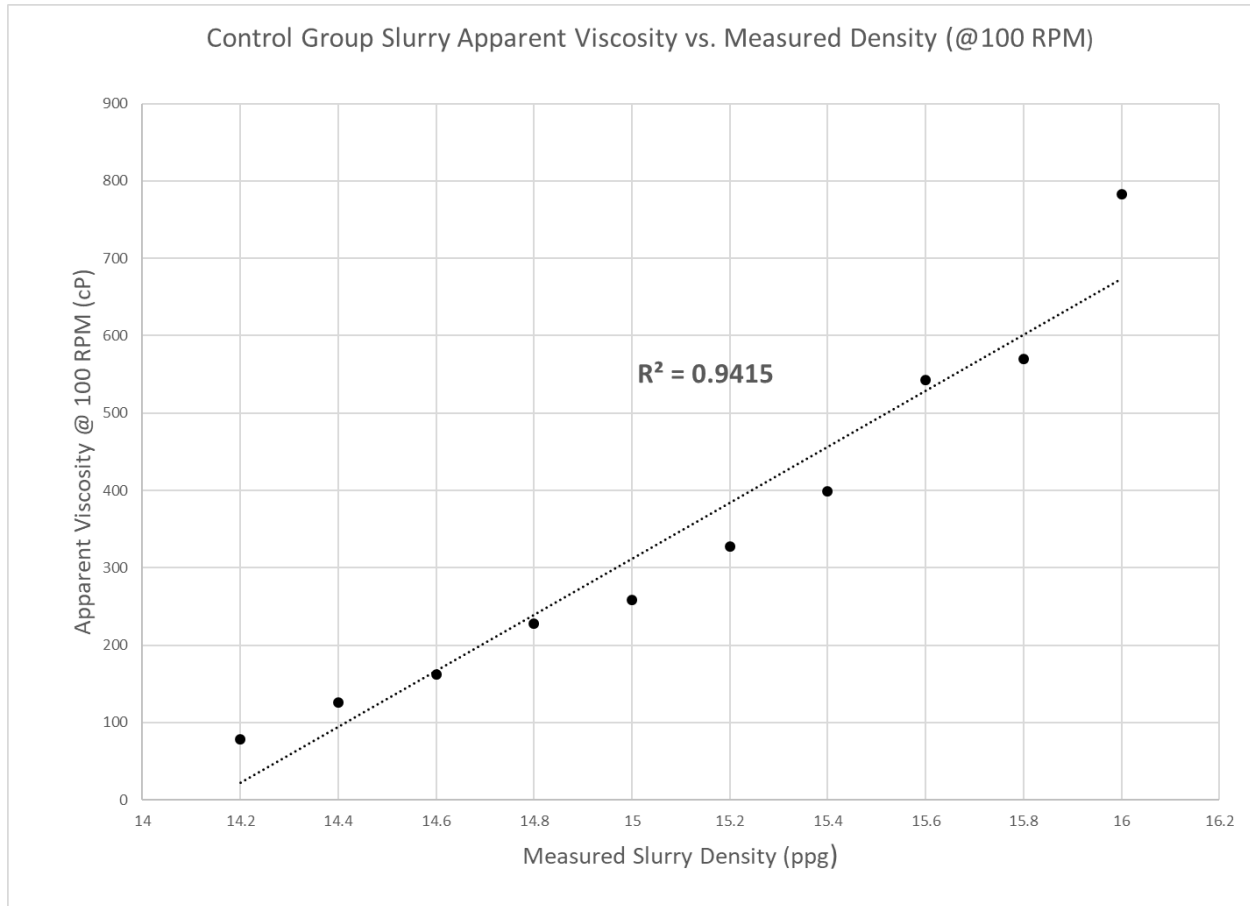


**Figure 23: Control Group Slurry Apparent Viscosity vs. Measured Density (@100 RPM)**

As the measured cement density increases, the apparent viscosity of the slurry also increases. This data set provides a base line in which to compare with the novel cement designs to observe the rheological effects of the addition of the novel materials to the cement design. Figure 24 displays the gel strength of the control group designs in relation to their measured slurry densities. While gel strength is equal to the dial deflection multiplied by a conversion factor of  $1.067 \text{ lb}_f./100 \text{ ft.}^2$ , for this study the assumption was made that dial deflection is equal to the gel strength in  $\text{lb}_f./100 \text{ ft.}^2$  since the conversion would only have a negligible effect on the data in this study.

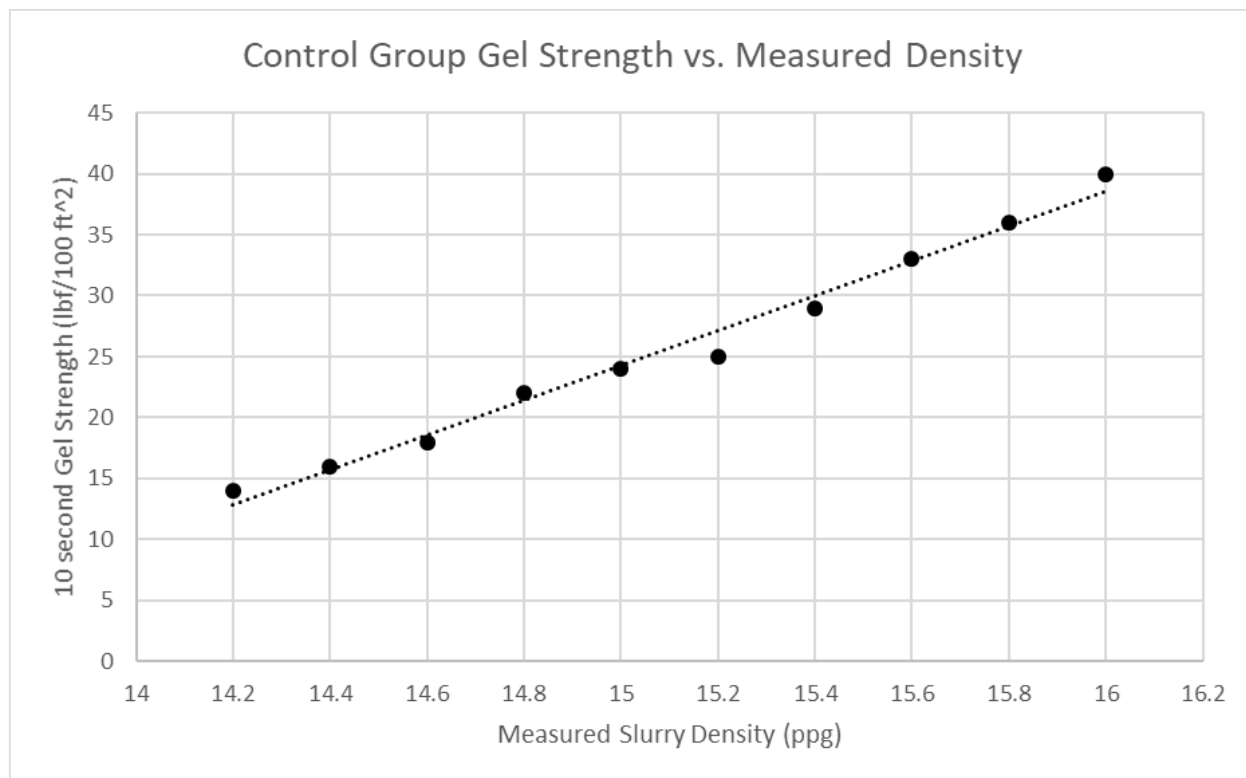


**Figure 24: Control Group Gel Strength vs. Measured Density Chart**

Similar to the apparent viscosity's relationship with slurry density in the control group designs, gel strength also increases as slurry density increases. This data set provides an adequate baseline to compare with rheological results of the novel cement designs.

#### **4.2.2. Hemp Hurd Rheological Testing Results**

This section contains the results of rheological testing of the 1-20 and 1-16 hemp hurd cement designs in this study. Ten cement designs were established for testing the 1-20 and 1-16 hemp hurd additives. Upon experimentation, it was discovered that at larger additive rates, fluid viscosity of the cement slurry was too high to be effectively measured by the Fann 35A Rotary Viscometer. Testing of these higher additive cement slurries resulted in erratic readings.

Due to this constraint, the following additive rates were tested for rheological properties for the 1-20 hurd additive: 0.25 lbs./sk, 0.5 lbs./sk, 1.0 lbs./sk, 1.5 lbs./sk, 2.0 lbs./sk, and 2.5 lbs./sk. The following additive rates were tested for rheological properties for the 1-16 hemp hurd additive: 0.25 lbs./sk, 0.5 lbs./sk, 1.0 lbs./sk, 1.5 lbs./sk, and 2.0 lbs./sk. The maximum dial deflection reading on the Fann Model 35A Rotary Viscometer is 300. Several measurements were taken at this maximum value. The readings for these samples will be listed as >300 in this work, but the author would like to note that the values could be larger and out of the measuring capability of the equipment used for the study.

Figure 25 displays apparent viscosity values of the 1-20 and 1-16 hemp hurd additive designs at 100 RPM in relation to cement slurry density. The control group data is also provided to compare with the novel designs.

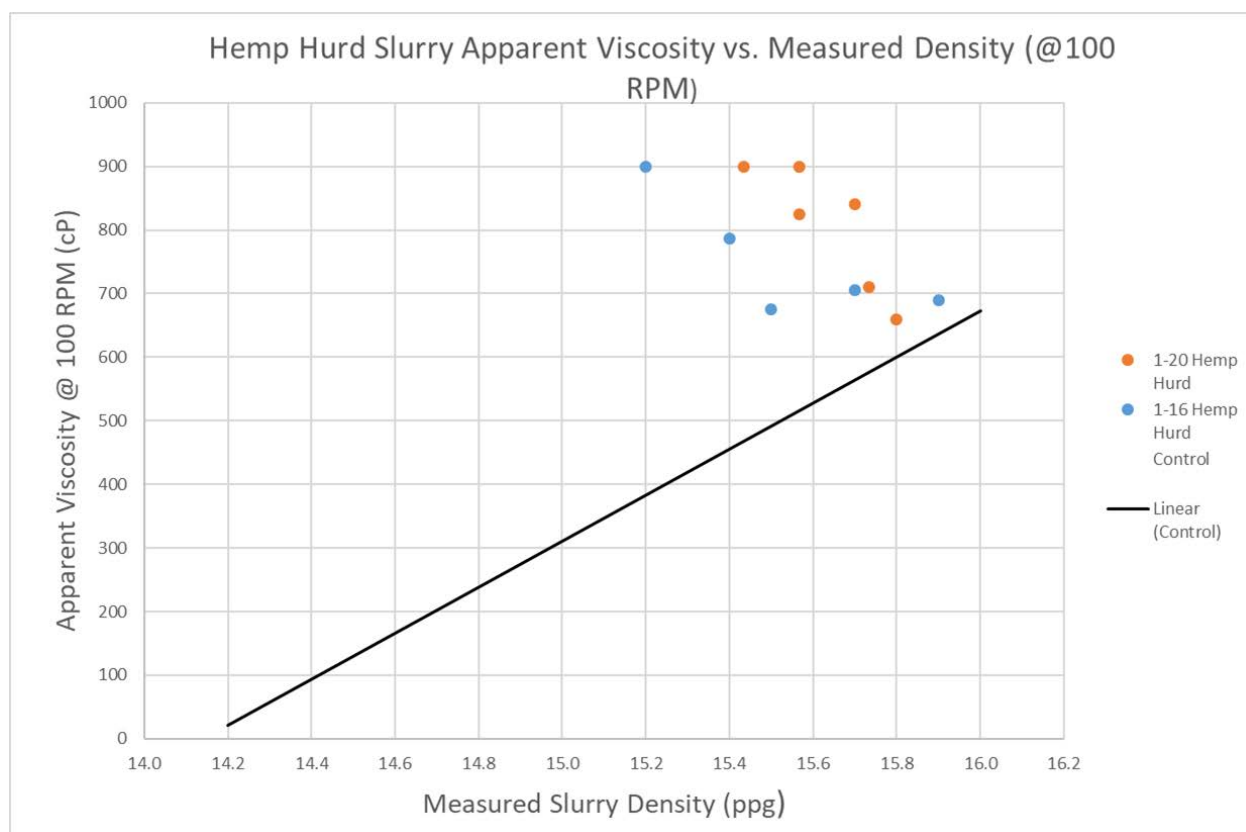


**Figure 25: Hemp Hurd Slurry Apparent Viscosity vs. Measured Density (@100 RPM)**



At matching cement slurry densities, the novel cement additive designs using both hemp hurd additives produce a large increase in apparent viscosity compared to the control group. The apparent viscosity of the hemp hurd samples also increases with a decrease in measured cement slurry density. This is due to a larger amount of hemp hurd additive present in the slurry at lower cement densities.

Gel strength also increases substantially with the two hemp hurd materials in comparison to the control group. This is displayed in Figure 26. Gel strength also increases with decreased cement density in the hemp hurd samples similar to the apparent viscosity.

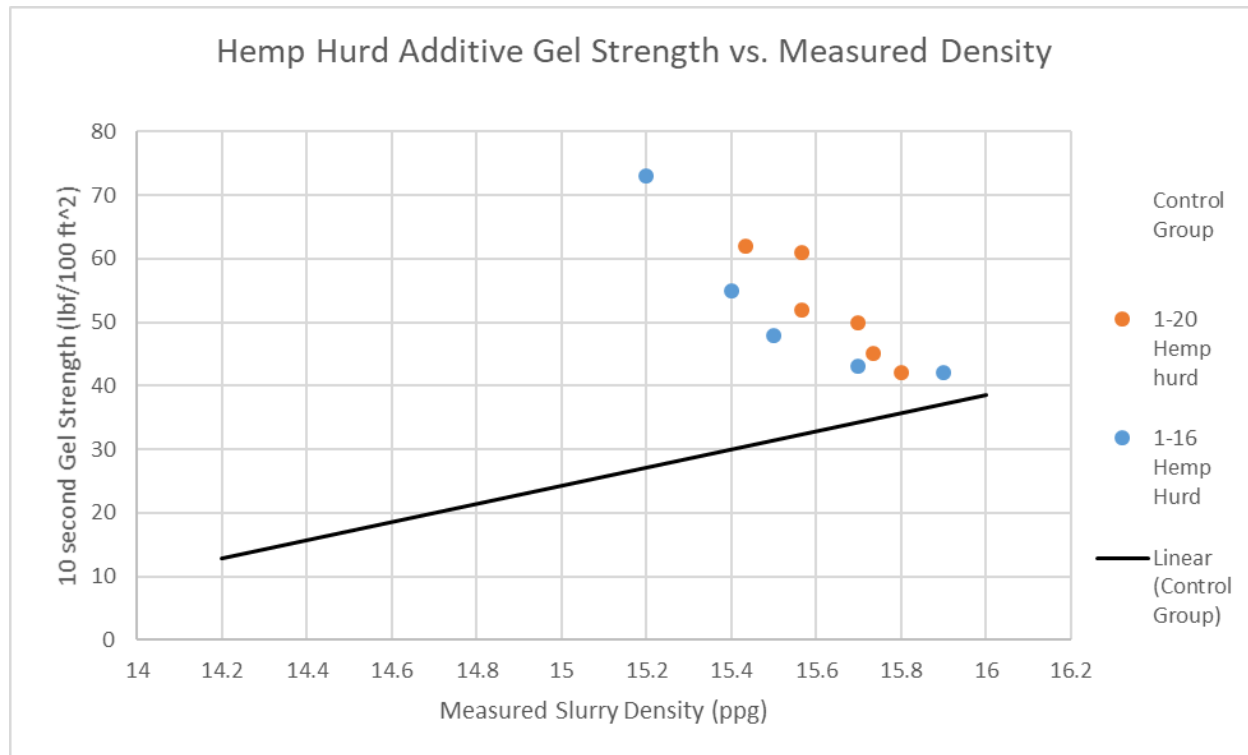


Figure 26: Hemp Hurd Additive Gel Strength vs. Measured Density

### 4.2.3. Biochar Rheological Property Testing Results

This section contains the results of rheological testing of the biochar additive cement designs in this study. Fourteen cement designs were established for testing the biochar additives

for rheological properties. These fourteen designs utilized the following biochar additive rates: 0.25 lbs./sk, 0.5 lbs./sk, 1.0 lbs./sk, 1.5 lbs./sk, 2.0 lbs./sk, 2.5 lbs./sk, 3.0 lbs./sk, 4.0 lbs./sk, 5.0 lbs./sk, 6.0 lbs./sk, 7.0 lbs./sk, 8.0 lbs./sk, 9.0 lbs./sk, and 10.0 lbs./sk. Figure 28 displays apparent viscosity values of the biochar additive designs at 100 RPM in relation to cement slurry density. The control group data is also provided to compare with the novel designs.

At slurry density values at and above 15.8 lbs./gal (118.2 lbs./ft.<sup>3</sup>), the biochar slurry has very similar apparent viscosity values compared with the control group values. At slurry density values below 15.8 lbs./gal., the biochar additive slurry produces a slightly higher apparent viscosity compared to control sample at matching cement slurry densities. The magnitude of increased apparent viscosity remains around 100 cp higher for the biochar additive slurry compared to the control slurry between densities of 15.1 lbs./gal. (112.9 lbs./ft.<sup>3</sup>) and 15.6 lbs./gal. (116.7 lbs./ft.<sup>3</sup>).

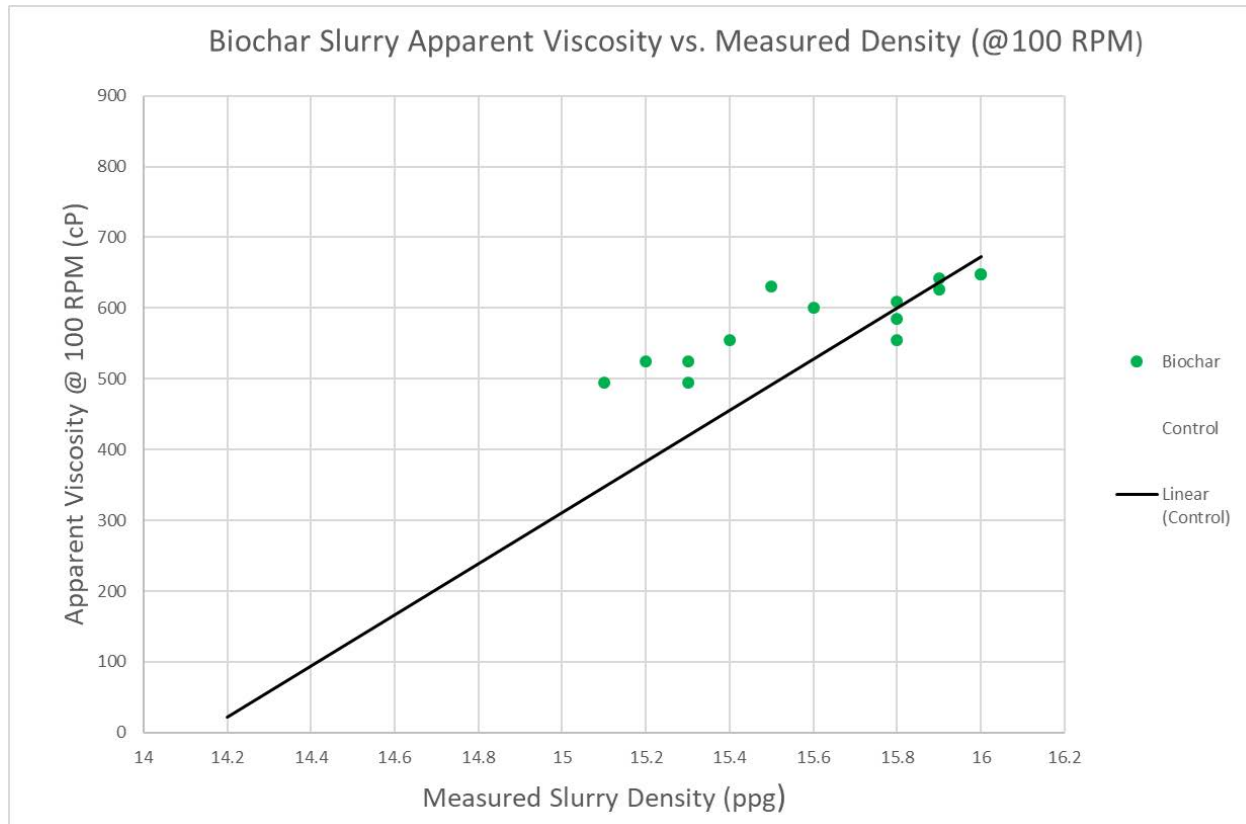


**Figure 28: Biochar Slurry Apparent Viscosity vs. Measured Density (@ 100 RPM)**

Figure 29 displays the gel strength of the cement slurries containing biochar additive.

The figure also displays the baseline control group values of gel strength.

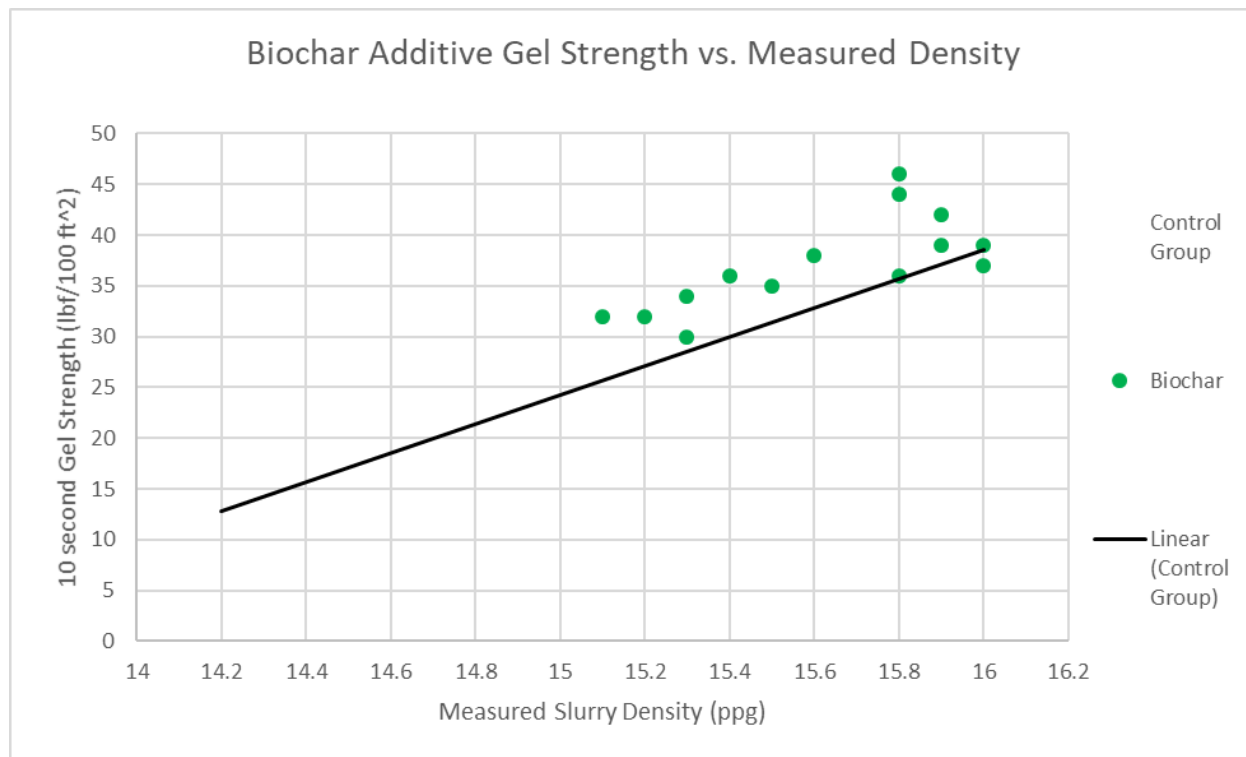


**Figure 29: Biochar Additive Gel Strength vs. Measured Density**

Throughout the entire range of slurry densities, it appears that the biochar slurries have an elevated gel strength in comparison to the control group. This increase remains relatively constant throughout the range of densities at a magnitude of approximately 4 lb<sub>f</sub>/100 ft.<sup>2</sup>.

#### 4.2.4. Non-Recyclable Plastic Rheological Testing Results

This section contains the results of rheological testing of the non-recyclable plastic additive cement designs in this study. Ten cement designs were established for testing the non-recyclable plastic additives for rheological properties. These ten designs utilized the following non-recyclable plastic additive rates: 0.25 lbs./sk, 0.5 lbs./sk, 1.0 lbs./sk, 1.5 lbs./sk, 2.0 lbs./sk,

2.5 lbs./sk, 3.0 lbs./sk, 4.0 lbs./sk, 5.0 lbs./sk, and 6.0 lbs./sk. During experimentation, it was observed that the non-recyclable plastic material was producing erratic rheometer readings at high additive rates. This is most likely attributed to the physical characteristics of the material. The material is square in shape with a very thin thickness, so it is possible that the material was adhering to the sides of the bob and sleeve mechanism of the rotary viscometer, which would produce inconsistent readings. Figure 30 displays apparent viscosity values of the non-recyclable plastic additive designs at 100 RPM in relation to cement slurry density. The control group data is also provided to compare with the novel designs.

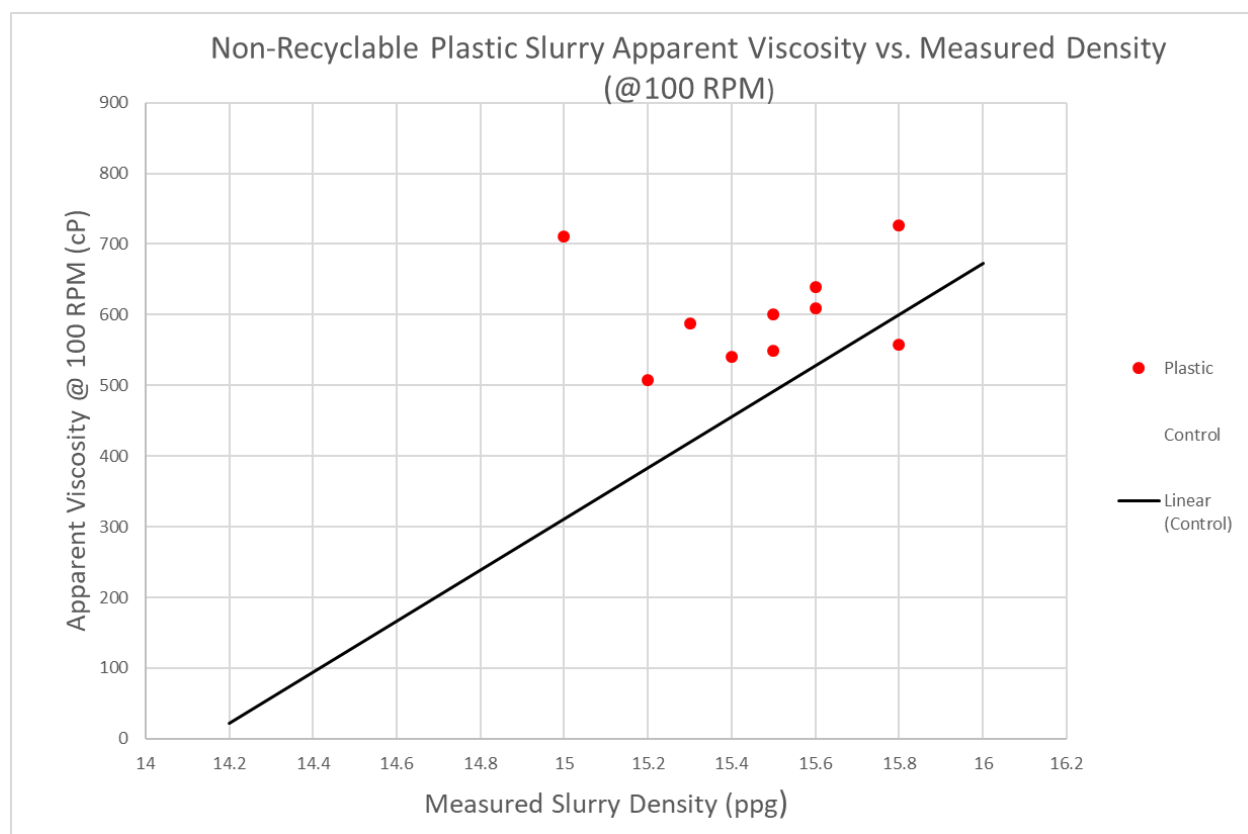


**Figure 30: Non-Recyclable Plastic Slurry Apparent Viscosity vs. Measured Density (@100 RPM)**

The non-recyclable plastic additive slurries increase in apparent viscosity as density increases in a similar fashion to the control group. At densities between 15.2 and 15.8 lbs./gal.

(113.7 lbs./ft.<sup>3</sup> and 118.2 lbs./ft.<sup>3</sup>), the slurries containing non-recyclable plastic tend to have an apparent viscosity of approximately 70 cp higher than the control group at matching cement slurry densities. The apparent viscosity value for the non-recyclable plastic at 15.0 lbs./gal. (112.2 lbs./ft.<sup>3</sup>) density has a high value and does not following the trend of the data. This could be attributed to the erratic rheometer readings described in this section. Figure 31 displays the relationship between the 10 second gel strength of the non-recyclable plastic cement design and the cement slurry density. The control group data is also provided to compare with the novel designs.

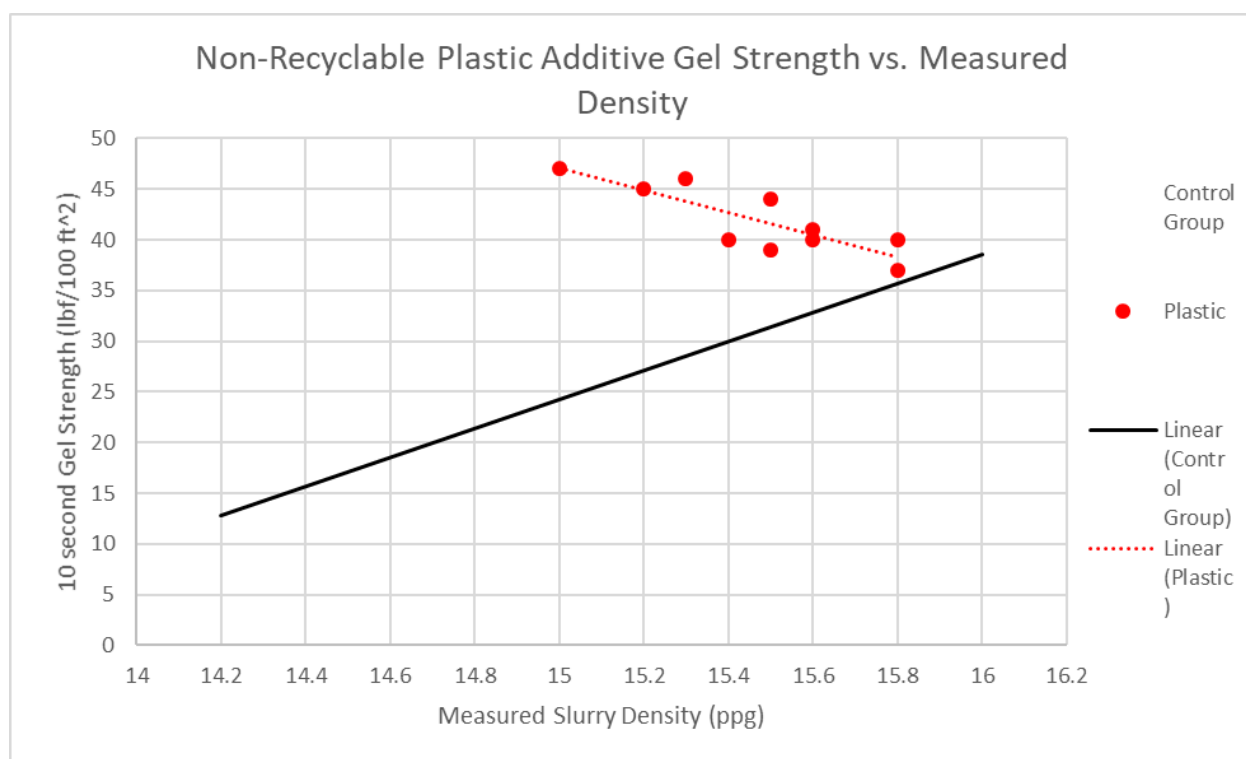


**Figure 31: Biochar Additive Gel Strength vs. Measured Density**

The non-recyclable plastic slurries increase in gel strength as slurry density decreases. A trendline was added to this data set to show this trend. This is most likely due to the increased amount of plastic in the lower cement density slurries. The higher concentration of the additive

in the low density slurries causes greater friction between the additive particles, which increases the slurry's apparent viscosity.

## 5. Discussion and Conclusions

The first section of this chapter analyses the results of the compressive strength and rheological testing experiments in this study. The next section of this chapter details the carbon sequestration potential of the proposed novel cement additives. The final portion of this chapter presents a concluding analysis of the novel carbon-storing materials as oilfield cementing additives.

### 5.1. Analysis of Unconfined Compressive Strength Results

This section is presented to discuss and analyze the results of the unconfined compressive strength experimentation utilizing hemp hurd, biochar, and non-recyclable plastics.

#### 5.1.1. Hemp Hurd Additive Unconfined Compressive Strength Analysis

Two grades of hemp hurd were introduced in cement designs that were constructed and tested for unconfined compressive strength after a curing period of 12 hours. The use of both of the hemp hurd size grades resulted in higher unconfined compressive strengths compared to the control designs at matching slurry densities (Figure 18). For example, at a slurry density value of 14.8 lbs./gal (110.7 lbs./ft<sup>3</sup>), the control cement produced an average unconfined compressive strength of 950 psi, whereas the 1-20 hemp hurd additive design at a 14.8 lbs./gal (110.7 lbs./ft<sup>3</sup>) slurry density produced an average unconfined compressive strength of 1219 psi. This is a 28.3% increase in the average compressive strength of the design at 14.8 lbs./gal (110.7 lbs./ft<sup>3</sup>) when the modified cement design using 1-20 Hemp Hurd is utilized compared to the control cement design.

This increase in compressive strength with the implementation of hemp hurd to the cement design can most likely be attributed to several factors. The first factor is that in the modified cement design, there is a slightly higher dry cement to water ratio. This is required,

since the hemp hurd is decreasing the density of the cement design, additional water must be utilized in the control design to achieve a decrease in cement slurry density. This is also a contributing factor when analyzing the biochar and non-recyclable plastic designs as well. Only a fraction of the water used in a cement slurry actually reacts with the cement material. The majority of the water in the design is used to create a flowable slurry. This additional water is then evaporated as the cement cures due to the exothermic reactions of the cement curing process. The water that is unused during the chemical reactions of the cement form pores in the cement, which decrease the cement's strength. By reducing the amount of water in the cement slurry, fewer pores are created and thus higher cement strengths are achieved. This is known as accelerated cement hydration. The higher dry cement to water ratio causes accelerated cement hydration, which increases early compressive strength. Additional acceleration of cement hydration is possibly caused by the hemp hurd additive itself. Hemp hurd is a highly porous absorbent material. This likely causes the hurd to absorb water during cement mixing and thus increases the dry cement to water ratio in the design, which then creates additional accelerated cement hydration. The third and last possible theory of added unconfined compressive strength is that the hemp hurd itself adds compressive strength to the cement.

### **5.1.2. Biochar Additive Unconfined Compressive Strength Analysis**

Biochar additive was introduced in cement designs that were constructed and tested for unconfined compressive strength after a curing period of 12 hours. The use of the modified cement design incorporating biochar resulted in higher unconfined compressive strengths compared to the control designs at matching slurry densities between 15.5 lbs./gal. (115.9 lbs./ft.<sup>3</sup>) and 16.0 lbs./gal. (119.7 lbs./ft.<sup>3</sup>) and produced similar compressive strength results as the control experiments at slurry densities below 15.5 lbs./gal. (115.9 lbs./ft.<sup>3</sup>) (Figure 20). At



slurry densities between 15.5 lbs./gal. (115.9 lbs./ft.<sup>3</sup>) and 16.0 lbs./gal. (119.7 lbs./ft.<sup>3</sup>), the modified cement design achieved unconfined compressive strengths approximately 10-20% greater than the control design at the same slurry density.

This initial increase in unconfined compressive strength utilizing the biochar additive can be most likely attributed by accelerated cement hydration. Similar to hemp hurd, biochar is considered to be a highly absorbent material. Absorption of water by the biochar material would increase the dry cement to water ratio, causing accelerated cement hydration and subsequently higher early compressive strength.

The loss of additional compressive strength gains at additive rates above 5 lbs./sk is hypothesized to be caused by the biochar becoming a major structural component of the cement.

### **5.1.3. Non-Recyclable Plastic Additive Unconfined Compressive Strength Analysis**

Non-recyclable plastic additive was introduced in cement designs that were constructed and tested for unconfined compressive strength after a curing period of 12 hours. The results of experimentation showed that the modified cement design using non-recyclable plastic produced very similar results to the control design at similar slurry densities (Figure 22). This would indicate that the non-recyclable plastic material did not have any substantial effect on the cement's compressive strength.

## **5.2. Analysis of Rheological Effects of the Novel Cement Additives**

This section is presented to discuss and analyze the results of the rheological experimentation utilizing hemp hurd, biochar, and non-recyclable plastics.

Rheological analysis of the hemp hurd additives utilized in the modified cement designs resulted in large viscosity increases with high concentrations of hemp hurd additive (Figure 25). The viscosity of the slurry was such that the Fann Model 35A Rotary Viscometer produced

maximum 100 RPM readings at a 2.0 lbs./sk 1-16 hemp hurd additive rate. Testing of the hemp hurd additive slurries were eliminated at additive rates above 2.5 lbs./sk due to viscosities above the measurement threshold of the Fann Model 35A Rotary Viscometer. A different apparatus would be required to test the viscosity values of cement slurries with higher concentrations of hemp hurd additive. The extreme increase in slurry viscosity is possibly caused by two main factors. The first factor is the increase in internal friction of the mixture caused by the fibrous hemp hurd material in the mixture. The second factor is the loss of mix water that is absorbed by the hemp hurd additive. Less mix water in a cement slurry leads to a higher viscosity cement. These high viscosity values could be a limiting factor to the amount of hemp hurd additive that can be suitably used in oilfield cementing applications.

Rheological analysis of the biochar additive in the modified cement design resulted in similar viscosities to the control group at similar slurry densities above 15.8 lbs./gal. (118.2 lbs./ft.<sup>3</sup>) and slightly higher viscosity values than the control group at similar slurry densities below 15.8 lbs./gal. (118.2 lbs./ft.<sup>3</sup>). During experimentation, it was observed that the biochar additive mixed very well into the cement slurry. This is most likely the cause of the additive having only slightly higher viscosity values in comparison to the control. The cause for the slight increase in viscosity at the higher additive rate is most likely attributed to the increased friction in the slurry caused by the presence of the particulate additive in the cement slurry. The slight increase in viscosity should not hinder most oilfield cementing operations, but it should be considered in applications where available pump horsepower is limited or situations where higher ECDs are problematic.

Rheological analysis of the non-recyclable plastic additive in the modified cement design resulted in viscosity values slightly higher than the control designs at similar cement slurry

densities (Figure 30). This slight increase is most likely attributed to the increased internal friction of the slurry caused by the presence of the impermeable non-recyclable plastic particles. This slight increase in viscosity should not hinder most oilfield cementing operations, but it should be considered in applications where available pump horsepower is limited or situations where higher ECDs are problematic.

### **5.2.1. Effects of Novel Cement Additives on Pump Pressure during a Primary Cementing Operation**

A surface casing cementing operation was simulated using K&M Technology Group's Extended Reach Architect (ERA) software platform to observe the pumping pressures associated with the use of the novel cement additives. The casing string was set at 5000 feet Measured Depth (MD) with no wellbore inclinations. The annular clearance between the outside of the casing and the wellbore was set at 1 inch. The rheological data for the control group slurry at 15.6 lbs./gal. (116.7 lbs./ft.<sup>3</sup>) was set as the base case to compare the novel additive designs with. The novel additive designs which produced 15.6 lbs./gal. (116.7 lbs./ft.<sup>3</sup>) slurry densities were selected to simulate in the cementing operation. The rheological data recorded during experimentation was used to model the different slurries containing the novel additives.

The use of the 15.6 lbs./gal. control group cement resulted in a maximum standpipe pressure of 3759 psi. The use of the 15.6 lbs./gal. (116.7 lbs./ft.<sup>3</sup>) 1-16 hemp hurd cement design (1.0 lbs./sk additive rate) resulted in a maximum standpipe pressure of 4946 psi, a 31.6% increase compared to the control. The use of the 15.6 lbs./gal. (116.7 lbs./ft.<sup>3</sup>) biochar cement design (4.0 lbs./sk additive rate) resulted in a maximum standpipe pressure of 3772 psi, which is a less than 1% increase compared to the control. The use of the 15.6 lbs./gal. (116.7 lbs./ft.<sup>3</sup>) non-recyclable plastic cement design (1.0 lbs./sk additive rate) resulted in a maximum standpipe pressure of 3773 psi, which is a less than 1% increase compared to the control.

The results of this simulation suggest that the effects of the biochar and non-recyclable plastic additives on slurry rheology are negligible in most common oilfield cementing applications. The results of the simulation also suggest that pumping cement designs using the novel hemp hurd additive could be very problematic at higher additive concentrations.

### **5.3. Carbon Sequestration Potential of Novel Cement Additives**

Research into the Life Cycle Assessment (LCA) of hemp hurd has determined that for every 1 lb. of hemp hurd stored, 1.84 lbs. of carbon dioxide equivalent is sequestered (Arhart et al., 2020). This is calculated based on the amount of carbon dioxide utilized by the hemp plant in its lifespan for photosynthesis. A slurry design utilizing 2.0 lbs./sk of hemp hurd sequesters 3.68 lbs. of carbon dioxide equivalent per sack of cement.

According to previous research, biochar has a carbon content by mass of around 85% (Basu, 2018). Since the source feed material for the biochar in this study is unknown, any carbon sequestered by the organic matter during its lifespan cannot be accounted for in this study. The only sequestered carbon that can be determined for the biochar in this study is its own carbon content by mass. This would correlate to 0.85 lbs. of sequestered carbon for every 1.0 lb of biochar stored in cement, resulting in 1.70 lbs. of carbon dioxide equivalent sequestered per sack of cement in a mixture consisting of 2.0 lbs./sk biochar.

According to the Global Alliance for Incinerator Alternatives, 2.9 lbs. of CO<sub>2</sub>e are emitted into the atmosphere for every 1 lb. of plastic that is incinerated. The primary disposal methods for non-recyclable plastics are storage in a landfill and incineration. To quantify the amount of carbon equivalent sequestered by storing the non-recyclable plastic, this study uses the assumption that the carbon storage potential non-recyclable plastic provides is the prevention from disposal by means of incineration, thus, the 2.9 lb. CO<sub>2</sub>e per lb. plastic ratio was utilized. A

slurry design utilizing 2.0 lbs./sk of non-recyclable plastic additive would sequester 5.8 lbs. of carbon dioxide equivalent per sack of cement utilized.

To put the carbon storage potential of the proposed novel additives into an oilfield application, Figure 32 displays the amount of carbon dioxide equivalent sequestered in each modified cement design based on the cumulative primary cementing operations conducted on a typical 20,000' measured depth horizontal onshore U.S. oil well. The primary cementing jobs on these types of wells typically utilize a total of approximately 2,000 sacks of cement.

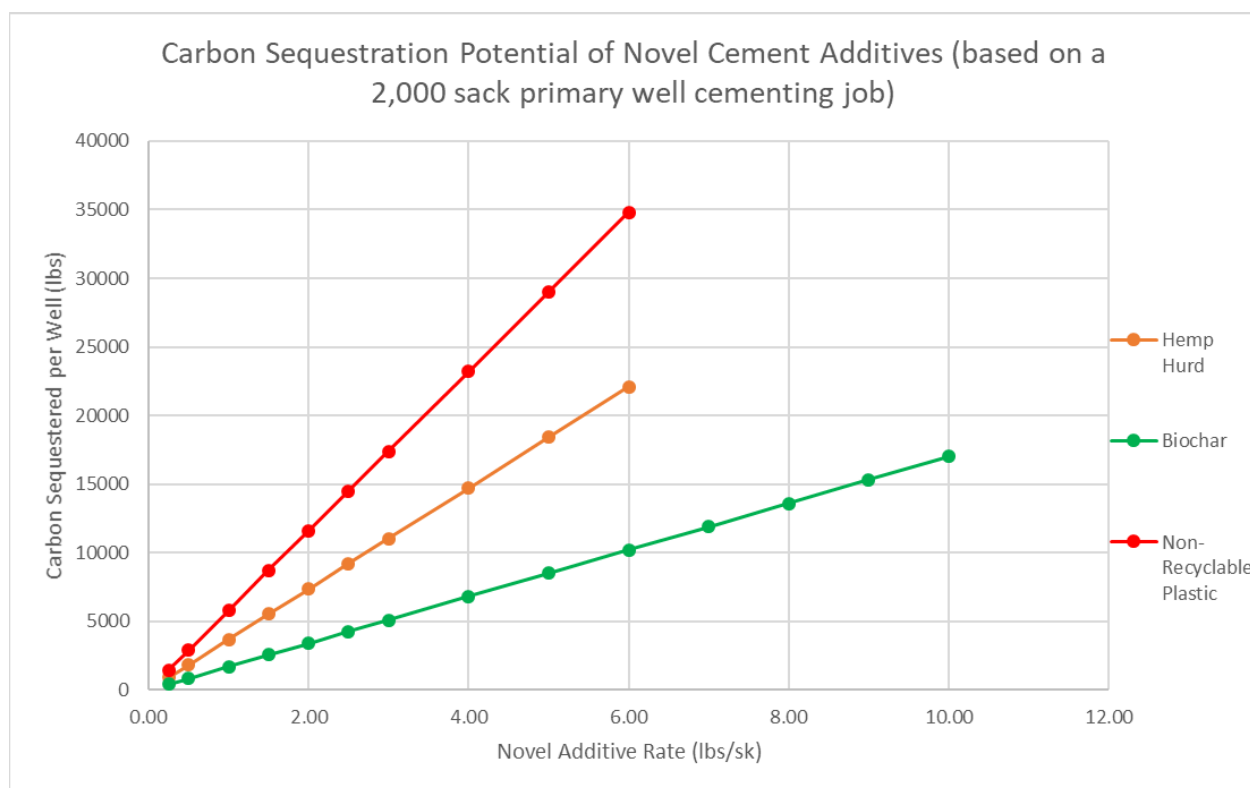


**Figure 32: Carbon Sequestration Potential of Novel Cement Additives**

Approximately 22,600 oil and gas wells were drilled in the U.S. in 2022. Assuming that 2,000 total sacks of cement were used in the primary cement jobs on these wells, utilizing a 2.0 lbs./sk hemp hurd additive in these well cementing operations would sequester almost 84,000 tons of carbon dioxide equivalent. Using the same assumptions, utilizing a 2.0 lbs./sk biochar

additive in these well cementing operations would sequester almost 39,000 tons of carbon dioxide equivalent. Utilizing a 2.0 lbs./sack non-recyclable plastic additive in these well cementing operations would sequester nearly 132,000 tons of carbon dioxide equivalent.

#### **5.4. Potential of Proposed Novel Materials as Oilfield Cement Additives**

This section analyses the practical applications of the novel carbon-storing additives presented in this work. While the main purpose of these materials in this study is storage of carbon, other characteristics the additive brings to the cement design could either promote or hinder its usage in the field. This section outlines the effects that these novel cement additives have when implemented in real world cementing applications.

##### **5.4.1. Hemp Hurd**

Through experimentation and analysis performed in this study, several favorable characteristics were identified when utilizing the hemp hurd additives in an oilfield cement design. The ability of the hemp hurd additive to accelerate cement hydration results in the achievement of higher early compressive strength. This is very favorable to most oilfield cementing applications as it decreases the required wait time to allow the cement to strengthen. In addition to sequestering carbon within the cement matrix, the fibrous structure of the hemp hurd material could potentially be used as a lost circulation material for primary oilfield cement. It is possible that the increase in viscosity resultant from additions of hemp hurd in cement slurries could cause pumpability and ECD issues when cementing longer intervals or where formation integrity is a concern.

##### **5.4.2. Biochar**

Through experimentation and analysis in this study, several favorable characteristics were identified when utilizing the biochar additive in an oilfield cement design. The addition of

biochar additive to the cement design displayed additional early compressive strength at additive rates up to 5.0 lbs./sk. This is very favorable to most oilfield cementing applications as it decreases the required wait time to allow the cement to reach desired strength values. The use of biochar in the cement design also displayed only a minimal effect on the slurry's viscosity. This minimal effect on slurry viscosity suggests that the novel additive could be implemented at high concentrations in most cementing applications without causing pumpability or ECD issues when cementing longer intervals or where formation integrity is a concern.

#### **5.4.3. Non-Recyclable Plastic**

Through experimentation and analysis in this study, several favorable characteristics were identified when utilizing the non-recyclable plastic additive in an oilfield cement design. Compressive strengths of cement samples containing the novel additive were not compromised with the addition of the novel additive. In addition to sequestering carbon within the cement matrix, the impermeable structure of the non-recyclable plastic material could potentially be used as a lost circulation material for primary oilfield cement. The use of non-recyclable plastic in the cement design also displayed only a minimal effect on the slurry's viscosity. This minimal effect on slurry viscosity suggests that the novel additive could be implemented at high concentrations in most cementing applications without causing pumpability or ECD issues when cementing longer intervals or where formation integrity is a concern. The non-recyclable plastic additive was also found to have the highest rate of carbon sequestration by mass out of the three materials.

## 6. Conclusions Overview

The following bullets summarize the conclusions regarding this study.

- The novel hemp hurd additive produced increased early compressive strength in cement samples at matching slurry densities, indicating the material may provide added value as a cement accelerator.
- The novel hemp hurd additive produced a significantly higher slurry viscosity when added into the design, which could hinder implementation in some oilfield cementing applications due to pumpability concerns.
- The novel biochar additive produced increased early compressive strength in cement samples at matching slurry densities at additive rates up to 6.0 lbs./sack, indicating the material may provide added value as a cement accelerator.
- The novel biochar additive had minimal effects on the cement slurry's apparent viscosity. This indicates that pumpability should not be an issue when implementing the additive in most oilfield cementing applications.
- The novel non-recyclable plastic additive had negligible effects on the cement's early compressive strength.
- The novel non-recyclable plastic additive had minimal effects on the cement slurry's apparent viscosity. This indicates that pumpability should not be an issue when implementing the additive in most oilfield cementing applications.
- The novel non-recyclable plastic additive had the highest carbon sequestration potential by mass out of the three proposed additives. The use of this additive at a rate of 6.0 lbs./sack (maximum rate for the material in this study) in a typical 2,000 sack well cementing operation would sequester approximately 35,000 lbs. of CO<sub>2e</sub> per well.



## **7. Recommendations for Future Work**

This investigation into the introduction of hemp hurd, biochar, and non-recyclable plastic into oilfield cement designs as carbon-storing materials produced results favorable to their possible eventual implementation into oilfield cement designs. The base build with this research can now be expanded upon to further investigate these additives' performance in oilfield cement designs. The following sections outline some considerations for future work regarding the use of hemp hurd, biochar, and non-recyclable plastics as oilfield cement additives.

### **7.1. Unconfined Compressive Strength Testing at Reservoir Temperature and Pressure**

In this study, all compressive strength experimentation was conducted at atmospheric pressure and at a temperature of  $70^{\circ}\text{F} \pm 5^{\circ}\text{F}$ . While this was sufficient for comparative analysis in this study, understanding the effects of elevated pressure and temperature on the samples containing the three novel additives would be essential before implementing the additives in real world cement designs, where the slurries will be exposed to elevated temperatures and pressures encountered downhole. This experimentation could be done with an apparatus such as the Ofite Model 120-51 Twin Cell UCA. This apparatus has the ability to cure cement samples under constant simulated reservoir pressures and temperatures. This apparatus also uses a non-destructive method of obtaining compressive strength data. This allows for a continuous measurement of the compressive strength as the cement sample cures.

### **7.2. Thickening Time Testing**

Thickening time is an important cement characteristic in oilfield cementing operations. Cementing operations in the oilfield can take hours to complete before the cement is pumped to its designated wellbore position. If cement begins to thicken too fast, it can compromise pumping operations and may require well remediation to correct. The modified cement designs

utilizing the novel cement additives at various additive rates should be evaluated for thickening times. Due to the accelerated cement hydration observed with the use of hemp hurd and biochar in this study, the author believes that this could have a substantial effect on the thickening time of the cement slurry.

This analysis can be completed using a lab consistometer. Most lab consistometers made for testing well cements also have the capability of simulating reservoir pressures and temperatures. Changes in slurry rheology over the thickening time of the cement can also be recorded using a lab consistometer. Thickening time analysis using the novel cement additives would provide useful knowledge to understand the effects of the novel additives on this metric before implementing the novel additive cement designs in the field.

### **7.3. Long-Term Compressive Strength Testing**

The compressive strength analysis in this study aimed to observe the effects of the novel additives on early compressive strength. An investigation into the long-term effects of the additive on compressive strength would help to better understand the novel materials and better quantify the actual factors affecting the strength of the cement, specifically in regards to the effect of accelerated cement hydration, which would not be apparent in long terms testing. This would provide an understanding of any structural support or lack of structural support provided by the novel materials.

### **7.4. Lost Circulation Material (LCM) Capability Testing**

The hemp hurd and non-recyclable plastic novel materials observed in this study have characteristics that would appear to make the materials favorable as possible LCM additives. This is due to the hemp hurd's fibrous composition and the impermeability of the non-recyclable plastic material. Materials which are impermeable can be advantageous as LCM additives as

they can create a barrier between the cement slurry and a permeable geologic formation, which prevents leakage of wellbore cement into the surrounding formations. There are currently no API recommended practices for testing the capability of a LCM in a cement design to the author's knowledge. However, many studies have been conducted testing various materials as LCMs. If a study could be done testing hemp hurd and non-recyclable plastic as LCMs, a better knowledge of the material would be acquired. If either of the materials prove to be an effective LCM, this would add value to the material's use as a carbon-storing cement additive, as it would have an additional characteristic favorable to a cement additive.

### **7.5. Investigation of Thermal Conductivity Effects of the Non-Recyclable Plastic Novel Cement Additive**

In previous studies investigating plastic aggregate in concrete designs, researchers discovered that concrete samples with various concentrations of plastic aggregate had a thermal conductivity 35-65% lower than the control concrete (Basha et al., 2020). An investigation into the effects of non-recyclable plastic additive on oilfield cement design thermal conductivity would show if the same phenomenon is true with oilfield cementing applications. If the results of the investigation of this theory prove that non-recyclable plastic drastically decreases the thermal conductivity of oilfield cements, this would add tremendous value to the non-recyclable plastic novel additive as it could be used in thermal injection projects to decrease heat losses through the cement while at the same time sequestering carbon. This is a large economical concern with thermal projects as a large amount of heat that is injected down the wellbore is lost to surrounding geologic formations from thermal conductivity in the casing and cement.

## 8. Recommended Future Work Overview

The following bullets summarize the recommended future work regarding this study.

- Investigation of the effects of the novel cement additives on oilfield cement compressive strength at reservoir temperature and pressure.
- Investigation of the effects of the novel cement additives on the thickening time of oilfield cements.
- Investigation of the effects of the novel cement additives on the long-term compressive strength of oilfield cements.
- Investigation of the potential of the novel cement additives as lost circulation materials (LCM).
- Investigation of the thermal conductivity effects of the novel non-recyclable plastic additive on oilfield cements.

## References Cited

- Ahmad, M., Lee, S. S., Lim, J. E., Lee, S. E., Cho, J. S., Moon, D. H., Hashimoto, Y., & Ok, Y. S. (2014). Speciation and phytoavailability of lead and antimony in a small arms range soil amended with mussel shell, cow bone and biochar: EXAFS spectroscopy and chemical extractions. *Chemosphere*, *95*, 433–441.  
<https://doi.org/10.1016/j.chemosphere.2013.09.077>
- Anshassi, M., Sackles, H., & Townsend, T. G. (2021). A review of LCA assumptions impacting whether landfilling or incineration results in less greenhouse gas emissions. *Resources, Conservation and Recycling*, *174*, 105810.  
<https://doi.org/10.1016/J.RESCONREC.2021.105810>
- API RP10B-2, *Recommended practice for testing well cements*, 1<sup>st</sup> edition, July 2005
- Arehart, J. H., Nelson, W. S., & Srubar, W. V. (2020). On the theoretical carbon storage and carbon sequestration potential of hempcrete. *Journal of Cleaner Production*, *266*.  
<https://doi.org/10.1016/j.jclepro.2020.121846>
- Basha, S. I., Ali, M. R., Al-Dulaijan, S. U., & Maslehuddin, M. (2020). Mechanical and thermal properties of lightweight recycled plastic aggregate concrete. *Journal of Building Engineering*, *32*, 101710. <https://doi.org/10.1016/J.JOBE.2020.101710>
- Basu, P. (2018). Pyrolysis. *Biomass Gasification, Pyrolysis and Torrefaction: Practical Design and Theory*, 155–187. <https://doi.org/10.1016/B978-0-12-812992-0.00005-4>
- Blunden, J., & Boyer, T. (2021). State of the climate in 2020. *Bulletin of the American Meteorological Society*, *102*(8), 1–481.  
<https://doi.org/10.1175/2021BAMSSStateoftheClimate.1>
- Cantrell, K. B., Hunt, P. G., Uchimiya, M., Novak, J. M., & Ro, K. S. (2012). Impact of pyrolysis temperature and manure source on physicochemical characteristics of biochar. *Bioresource Technology*, *107*, 419–428. <https://doi.org/10.1016/j.biortech.2011.11.084>

- Das, O., Sarmah, A. K., & Bhattacharyya, D. (2015). A novel approach in organic waste utilization through biochar addition in wood/polypropylene composites. *Waste management*, 38, 132-140.
- Ellis, L. D., Badel, A. F., Chiang, M. L., Park, R. J. Y., & Chiang, Y. M. (2020). Toward electrochemical synthesis of cement—An electrolyzer-based process for decarbonating CaCO<sub>3</sub> while producing useful gas streams. *Proceedings of the National Academy of Sciences of the United States of America*, 117(23), 12584–12591.  
<https://doi.org/10.1073/pnas.1821673116>
- Gandolfi, S., Ottolina, G., Riva, S., Fantoni, G. P., and Patel, I. (2013). "Complete chemical analysis of Carmagnola hemp hurds and structural features of its components," *BioRes.* 8(2), 2641-2656.
- Gupta, S., & Kashani, A. (2021). Utilization of biochar from unwashed peanut shell in cementitious building materials—Effect on early age properties and environmental benefits. *Fuel Processing Technology*, 218, 106841.
- Gupta, S., Kua, H. W., & Cynthia, S. Y. T. (2017). Use of biochar-coated polypropylene fibers for carbon sequestration and physical improvement of mortar. *Cement and Concrete Composites*, 83, 171-187.
- Gupta, S., Kua, H. W., & Low, C. Y. (2018). Use of biochar as carbon sequestering additive in cement mortar. *Cement and concrete composites*, 87, 110-129.
- Jamaludin, N., Rashid, S. A., & Tan, T. (2019). Natural Biomass as Carbon Sources for the Synthesis of Photoluminescent Carbon Dots. *Synthesis, Technology and Applications of Carbon Nanomaterials*, 109–134. <https://doi.org/10.1016/B978-0-12-815757-2.00005-X>
- Jami, T., Karade, S. R., & Singh, L. P. (2019). A review of the properties of hemp concrete for green building applications. *Journal of Cleaner Production*, 239, 117852.  
<https://doi.org/10.1016/J.JCLEPRO.2019.117852>

- Jeon, J., Park, J. H., Yuk, H., Kim, Y. U., Yun, B. Y., Wi, S., & Kim, S. (2021). Evaluation of hygrothermal performance of wood-derived biocomposite with biochar in response to climate change. *Environmental Research*, *193*, 110359.
- Legan, M., Gotvajn, A. Ž., & Zupan, K. (2022). Potential of biochar use in building materials. *Journal of Environmental Management*, *309*, 114704. <https://doi.org/10.1016/J.JENVMAN.2022.114704>
- Li, X., Ling, T. C., & Hung Mo, K. (2020). Functions and impacts of plastic/rubber wastes as eco-friendly aggregate in concrete – A review. *Construction and Building Materials*, *240*, 117869. <https://doi.org/10.1016/J.CONBUILDMAT.2019.117869>
- Maagi, M. T., Lupyana, S. D., & Jun, G. (2020). Nanotechnology in the petroleum industry: Focus on the use of nanosilica in oil-well cementing applications - A review. *Journal of Petroleum Science and Engineering*, *193*, 107397. <https://doi.org/10.1016/J.PETROL.2020.107397>
- Praneeth, S., Saavedra, L., Zeng, M., Dubey, B. K., & Sarmah, A. K. (2021). Biochar admixed lightweight, porous and tougher cement mortars: Mechanical, durability and micro computed tomography analysis. *Science of The Total Environment*, *750*, 142327.
- Qin, Y., Pang, X., Tan, K., & Bao, T. (2021). Evaluation of pervious concrete performance with pulverized biochar as cement replacement. *Cement and Concrete Composites*, *119*, 104022.
- Rahman, M. M., Sultan, M. B., & Alam, M. (2023). Microplastics and adsorbed micropollutants as emerging contaminants in landfill: A mini review. *Current Opinion in Environmental Science & Health*, *31*, 100420. <https://doi.org/10.1016/J.COESH.2022.100420>
- Restuccia, L., & Ferro, G. A. (2016). Nanoparticles from food waste: a "green" future for traditional building materials. In *9th International Conference on Fracture Mechanics of Concrete and Concrete Structures FraMCoS-9*.

- Suarez-Riera, D., Restuccia, L., & Ferro, G. A. (2020). The use of Biochar to reduce the carbon footprint of cement-based materials. *Procedia Structural Integrity*, 26, 199-210.
- Sutton, A., Black, D., & Walker, P. (2011). *Straw bale: an introduction to low-impact building materials*. IHS BRE Press.
- Svante Arrhenius (1896). "On the influence of carbonic acid in the air upon the temperature of the ground". *Philosophical Magazine and Journal of Science*. **41** (251): 237–276. doi:10.1080/14786449608620846.
- Tayeh, B. A., Almeshal, I., Magbool, H. M., Alabduljabbar, H., & Alyousef, R. (2021). Performance of sustainable concrete containing different types of recycled plastic. *Journal of Cleaner Production*, 328, 129517.  
<https://doi.org/10.1016/J.JCLEPRO.2021.129517>
- Vrålstad, T., Saasen, A., Fjær, E., Øia, T., Ytrehus, J. D., & Khalifeh, M. (2019). Plug & abandonment of offshore wells: Ensuring long-term well integrity and cost-efficiency. *Journal of Petroleum Science and Engineering*, 173, 478–491.  
<https://doi.org/10.1016/J.PETROL.2018.10.049>
- Walker, R., Pavia, S., & Mitchell, R. (2014). Mechanical properties and durability of hemp-lime concretes. *Construction and Building Materials*, 61, 340–348.  
<https://doi.org/10.1016/j.conbuildmat.2014.02.065>
- Zeidabadi, Z. A., Bakhtiari, S., Abbaslou, H., & Ghanizadeh, A. R. (2018). Synthesis, characterization and evaluation of biochar from agricultural waste biomass for use in building materials. *Construction and Building Materials*, 181, 301-308.



## 9. Appendix A: Unconfined Compressive Strength Results

<b>12 Hour Compressive Strength Test Results - Control Group</b>		
<b>Sample</b>	<b>Compressive Strength (psi)</b>	<b>Measured Density (lbs./gal)</b>
1	2000	16.1
2	2050	
3	2125	
1	1850	15.8
2	2075	
3	2150	
1	1650	15.7
2	1600	
3	1875	
1	1350	15.4
2	1350	
3	1150	
1	1200	15.1
2	1275	
3	1225	
1	1075	14.9
2	1100	
3	1125	
1	950	14.8
2	1000	
3	900	
1	800	14.6
2	700	
3	850	
1	675	14.4
2	700	
3	675	
1	625	14.3
2	575	
3	600	

<b>12 Hour Compressive Strength Test Results - 1-20 Hemp Hurd Additive</b>		
<b>Sample</b>	<b>Compressive Strength (psi)</b>	<b>Measured Density (lbs./gal)</b>
<b>1/4 lbs./sk 1/20 Size Hemp Hurd Additive</b>		
1	1850	15.8
2	2000	
3	1800	
4	1800	15.8
5	1850	
6	1800	
7	1950	15.8
8	1975	
9	1850	
<b>1/2 lbs./sk 1/20 Size Hemp Hurd Additive</b>		
1	1650	15.7
2	1725	
3	1650	
4	1950	15.7
5	1825	
6	1875	
7	1850	15.8
8	1875	
9	1900	
<b>1 lbs./sk 1/20 Size Hemp Hurd Additive</b>		
1	1800	15.7
2	1950	
3	1650	
4	1675	15.7
5	1650	
6	1800	
7	1775	15.7
8	1650	
9	1850	
<b>1 1/2 lbs./sk 1/20 Size Hemp Hurd Additive</b>		

1	1650	15.5
2	1350	
3	2000	
4	1800	15.6
5	1800	
6	1850	
7	1825	15.6
8	1625	
9	1825	
<b>2 lbs./sk 1/20 Size Hemp Hurd Additive</b>		
1	1700	15.6
2	1950	
3	1825	
4	1650	15.6
5	1650	
6	1600	
7	1725	15.5
8	1800	
9	1800	
<b>2 1/2 lbs./sk 1/20 Size Hemp Hurd Additive</b>		
1	1750	15.4
2	1700	
3	1725	
4	1475	15.5
5	1600	
6	1725	
7	1850	15.4
8	1675	
9	1750	
<b>3 lbs./sk 1/20 Size Hemp Hurd Additive</b>		
1	1750	15.5
2	1450	
3	1400	
4	1450	15.4
5	1650	
6	1575	
7	1450	15.3
8	1425	

9	1425	
<b>4 lbs./sk 1/20 Size Hemp Hurd Additive</b>		
1	1300	15.3
2	1200	
3	1300	
4	1250	15.2
5	1300	
6	1300	
7	1400	15.3
8	1450	
9	1350	
<b>5 lbs./sk 1/20 Size Hemp Hurd Additive</b>		
1	1250	15.0
2	1300	
3	1450	
4	1400	15.1
5	1225	
6	1350	
7	1175	14.9
8	1300	
9	1275	
<b>6 lbs./sk 1/20 Size Hemp Hurd Additive</b>		
1	1325	14.9
2	1150	
3	1325	
4	1125	14.8
5	1250	
6	1225	
7	1125	14.7
8	1200	
9	1250	

<b>12 Hour Compressive Strength Test Results - 1-16 Hemp Hurd Additive</b>		
<b>Sample</b>	<b>Compressive Strength (psi)</b>	<b>Measured Density (lbs./gal)</b>
<b>0.25 lbs./sk 1-16 Hemp Hurd Additive</b>		
1	1800	15.9
2	1975	
3	2025	
<b>0.5 lbs./sk 1-16 Hemp Hurd Additive</b>		
1	1900	15.7
2	1900	
3	1975	
<b>1 lbs./sk 1-16 Hemp Hurd Additive</b>		
1	1675	15.5
2	1750	
3	1625	
<b>1.5 lbs./sk 1-16 Hemp Hurd Additive</b>		
1	1700	15.4
2	1675	
3	1675	
<b>2 lbs./sk 1-16 Hemp Hurd Additive</b>		
1	1625	15.2
2	1525	
3	1625	
<b>2.5 lbs./sk 1-16 Hemp Hurd Additive</b>		
1	1500	15.2
2	1600	
3	1550	
<b>3 lbs./sk 1-16 Hemp Hurd Additive</b>		
1	1475	15
2	1450	
3	1400	
<b>4 lbs./sk 1-16 Hemp Hurd Additive</b>		
1	1125	14.5
2	1225	

3	1225	
<b>5 lbs./sk 1-16 Hemp Hurd Additive</b>		
1	1050	14.3
2	1075	
3	1025	
<b>6 lbs./sk 1-16 Hemp Hurd Additive</b>		
1	950	14.1
2	1025	
3	950	

<b>12 Hour Compressive Strength Test Results - Biochar Additive</b>		
Sample	Compressive Strength (psi)	Measured Density (lbs./gal)
<b>0.25 lbs./sk Biochar Additive</b>		
1	2350	15.8
2	2225	
3	2150	
<b>0.5 lbs./sk Biochar Additive</b>		
1	2250	15.8
2	2250	
3	2275	
<b>1 lbs./sk Biochar Additive</b>		
1	2125	15.9
2	2150	
3	2150	
<b>1.5 lbs./sk Biochar Additive</b>		
1	2150	16.0
2	2050	
3	2250	
<b>2 lbs./sk Biochar Additive</b>		
1	2075	16
2	2275	
3	2225	
<b>2.5 lbs./sk Biochar Additive</b>		

1	2200	15.9
2	2200	
3	2075	
<b>3 lbs./sk Biochar Additive</b>		
1	2025	15.8
2	2375	
3	2275	
<b>4 lbs./sk Biochar Additive</b>		
1	2125	15.6
2	2075	
3	2025	
<b>5 lbs./sk Biochar Additive</b>		
1	2100	15.5
2	1950	
3	1850	
<b>6 lbs./sk Biochar Additive</b>		
1	1400	15.4
2	1450	
3	1550	
<b>7 lbs./sk Biochar Additive</b>		
1	1450	15.3
2	1425	
3	1400	
<b>8 lbs./sk Biochar Additive</b>		
1	1400	15.3
2	1375	
3	1450	
<b>9 lbs./sk Biochar Additive</b>		
1	1550	15.2
2	1500	
3	1500	
<b>10 lbs./sk Biochar Additive</b>		
1	1250	15.1
2	1250	
3	1275	

<b>12 Hour Compressive Strength Test Results - Plastic Additive</b>		
<b>Sample</b>	<b>Compressive Strength (psi)</b>	<b>Measured Density (lbs./gal)</b>
<b>0.25 lbs./sk Plastic Additive</b>		
1	1950	15.8
2	1850	
3	1800	
<b>0.5 lbs./sk Plastic Additive</b>		
1	1825	15.8
2	1950	
3	1850	
<b>1 lbs./sk Plastic Additive</b>		
1	1650	15.6
2	1625	
3	1700	
<b>1.5 lbs./sk Plastic Additive</b>		
1	1600	15.6
2	1550	
3	1625	
<b>2 lbs./sk Plastic Additive</b>		
1	1500	15.5
2	1550	
3	1550	
<b>2.5 lbs./sk Plastic Additive</b>		
1	1650	15.5
2	1650	
3	1500	
<b>3 lbs./sk Plastic Additive</b>		
1	1500	15.4
2	1500	
3	1450	
<b>4 lbs./sk Plastic Additive</b>		
1	1325	15.3
2	1450	
3	1500	
<b>5 lbs./sk Plastic Additive</b>		



1	1425	15.2
2	1325	
3	1300	
<b>6 lbs./sk Plastic Additive</b>		
1	1450	15
2	1500	
3	1250	

## 10. Appendix B: Water Requirement Calculation for Control Group Experiments

Due to density differences between the three observed novel additives, a control set of experiments with no novel additive and vary cement slurry density values was created to compare with the varying densities of the novel cement designs with the proposed additives. This was achieved by varying the amount of mix water to change the cement density of the original cement design to match the slurry densities created by the addition of varying amounts of novel additive. The original rounds of experimentation isolated the additive rate and type of novel additive as the only variable between each experiment. This is shown in the original cement design shown below:

Trident IL(10) Portland Limestone Cement

3% Calcium Chloride Mini Pellets

X lbs./sk Novel Cement Additive\*

5.0 gal/sk H<sub>2</sub>O

\*Varying amounts of this additive were used throughout lab testing.

In the control round of experimentation, novel materials would be excluded from the cement design, and the water mix rate would be varied to create varying cement slurry densities.

This new design is shown below:

Trident IL(10) Portland Limestone Cement

3% Calcium Chloride Mini Pellets

X gal/sk H<sub>2</sub>O

\*Varying amounts of this additive were used throughout lab testing.

Observed cement slurry densities from the previous rounds of testing ranged from 14.1 lbs./gal to 16.0 lbs./gal. To create an appropriate range of data to compare with previously

observed cement densities, 10 experiments were established to create the following calculated cement slurry densities: 14.0 lbs./gal, 14.2 lbs./gal, 14.4 lbs./gal, 14.6 lbs./gal, 14.8 lbs./gal, 15.0 lbs./gal, 15.2 lbs./gal, 15.4 lbs./gal, 15.6 lbs./gal, 15.8 lbs./gal, and 16.0 lbs./gal.

Achieving the desired cement densities in this round of experimentation can be done by calculating the amount of mix water required to change the slurry density to the target value. The method used to achieve this calculation is displayed in the following section.

## Water Requirement Calculation Example

Cement Formula:

Trident IL(10) Portland Cement

3% Calcium Chloride

X gal/sk water

Target Cement Density = 15.6 lbs./gal

Absolute Volume of each material is listed below:

Trident IL(10) Portland Cement = 0.0382 gal/lb

Calcium Chloride = 0.0558 gal/lb

Water = 0.1199 gal/lb

We can use the absolute volume values along with component weights in lb/sk in the following equation to solve for water volume:

Cement Density (lb/gal) = Total weight per sack of cement (lb/sk) / Total volume of cement slurry (gal/sk)

The following table displays to calculation steps to form the cement density equation:

	<b>Weight (lb/sk)</b>	<b>Absolute Volume (gal/lb)</b>	<b>Volume (Gal/sk)</b>
<b>1 sack of Trident IL(10) Portland Cement</b>	94	0.0382	$94 * 0.0382$ $= 3.591$
<b>3% Calcium Chloride</b>	$0.03 * 94 = 2.82$	0.0558	$2.82 *$ $0.0558 = 0.1574$
<b>Water</b>	$8.34 * k$	0.1199	k
<b>Total</b>	$94+2.82+(8.34*k)$	-	$3.591 +$ $0.1574 + k$

Where k = water volume in gal/sk

Insert values into Cement Density equation:

$$15.6 \text{ lbs./gal} = (94+2.82+(8.34*k))(\text{lb/sk}) / (3.591+0.1574+k)(\text{gal/sk})$$

Solve for k:

$$\underline{K = \text{Water Requirement} = 5.28 \text{ gal/sk}}$$

This method can be applied for each target cement density to be studied in the control round of experimentation.

## 11. Appendix C: 100 RPM Apparent Viscosity and Gel Strength Results

<b>Control Group Rheological Testing Results</b>				
<b>Slurr Density (ppg)</b>	<b>Shear Rate (rpm)</b>	<b>Deflection</b>	<b>Apparent Viscosity (cP)</b>	<b>Gel Strength (lbf/100 ft<sup>2</sup>)</b>
14.2	100	26	78	14
14.4	100	42	126	16
14.6	100	54	162	18
14.8	100	76	228	22
15.0	100	86	258	24
15.2	100	109	327	25
15.4	100	133	399	29
15.6	100	181	543	33
15.8	100	190	570	36
16	100	261	783	40

<b>1-20 Hemp Hurd Rheological Testing Results</b>					
<b>Additive Rate (lbs/sk)</b>	<b>Slurr Density (ppg)</b>	<b>Shear Rate (rpm)</b>	<b>Deflection</b>	<b>Apparent Viscosity (cP)</b>	<b>Gel Strength (lbf/100 ft<sup>2</sup>)</b>
0.25	15.8	100	220	660	42
0.50	15.7	100	237	711	45
1.00	15.7	100	280	840	50
1.50	15.6	100	275	825	52
2.00	15.6	100	300	900	61
2.50	15.4	100	300	900	62

<b>1-16 Hemp Hurd Rheological Testing Results</b>					
<b>Additive Rate (lbs/sk)</b>	<b>Slurr Density (ppg)</b>	<b>Shear Rate (rpm)</b>	<b>Deflection</b>	<b>Apparent Viscosity (cP)</b>	<b>Gel Strength (lbf/100 ft<sup>2</sup>)</b>
0.25	15.9	100	230	690	42
0.5	15.7	100	235	705	43
1	15.5	100	225	675	48
1.5	15.4	100	262	786	55
2	15.2	100	300	900	73

<b>Biochar Rheological Testing Results</b>					
<b>Additive Rate (lbs/sk)</b>	<b>Slurr Density (ppg)</b>	<b>Shear Rate (rpm)</b>	<b>Deflection</b>	<b>Apparent Viscosity (cP)</b>	<b>Gel Strength (lbf/100 ft<sup>2</sup>)</b>
0.25	15.8	100	185	555	46
0.5	15.8	100	203	609	44
1	15.9	100	209	627	42
1.5	16	100	216	648	39
2	16	100	216	648	37
2.5	15.9	100	214	642	39
3	15.8	100	195	585	36
4	15.6	100	200	600	38
5	15.5	100	210	630	35
6	15.4	100	185	555	36
7	15.3	100	165	495	30
8	15.3	100	175	525	34
9	15.2	100	175	525	32
10	15.1	100	165	495	32

<b>Non-Recyclable Plastic Rheological Testing Results</b>					
<b>Additive Rate (lbs/sk)</b>	<b>Slurr Density (ppg)</b>	<b>Shear Rate (rpm)</b>	<b>Deflection</b>	<b>Apparent Viscosity (cP)</b>	<b>Gel Strength (lbf/100 ft<sup>2</sup>)</b>
0.25	15.8	100	242	726	40
0.50	15.8	100	186	558	37
1.00	15.6	100	213	639	41
1.50	15.6	100	203	609	40
2.00	15.5	100	200	600	44
2.50	15.5	100	183	549	39
3.00	15.4	100	180	540	40
4.00	15.3	100	196	588	46
5.00	15.2	100	169	507	45
6.00	15	100	237	711	47